AN ABSTRACT OF THE THESIS OF

William John Schweller (Name) for the Master of Science (Degree)

in Oceanography (Major) presented on 27 February 1976 (Date)

Title: CHILE TRENCH: EXTENSIONAL RUPTURE OF OCEANIC CRUST AND THE INFLUENCE OF TECTONICS ON SEDIMENT DISTRIBUTION

Redacted for Privacy

Abstract approved: _____

L. D. Kulm

Extensive new trackline coverage of the Chile Trench between 23°S and 34°S, including more than 60 bathymetric and seismic reflection profiles across the trench axis, allows a much more detailed study of the tectonics and sedimentation of this feature than previously possible. Sediment distribution along the axis shows a remarkable variation from over a kilometer of turbidites in the axis south of 33°S to a barren axis in places north of 27°S. Turbidity currents originating on the outer continental margin in the south carry sediment northward along the axis. Ponding behind structural barriers created by plate convergence restricts the amount of sediment reaching northern trench sections.

Horst and graben blocks are the dominant structural features on the seaward trench slope, with fault offsets of 500 to 1000 meters.

Grabens range in width from 4 to 8 km, while the faulting probably extends down into oceanic layer three. Faulting is most pronounced in the deeper northern parts of the trench, but can also be seen in the basement beneath undeformed axial sediments in the south. This crustal rupture can be related to extensional stress in the upper oceanic crust due to the downbending of the Nazca Plate prior to subduction. Most of the active normal faulting occurs soon after the plate begins its descent into the trench, and not within the trench axis.

Using structure, sediment distribution, bathymetry, and morphology, the trench and outer continental margin can be divided into three provinces (Northern, 23°-27°S; Central 27°-33°S; and Southern, 33°-34°S) separated by distinct tectonic transition zones at 27°S and 33°S. These boundaries coincide with breaks in onshore geologic trends and correlate less well with seismic zone segmentation. An analysis of potential strain due to subduction along a non-arcuate trench concludes that segmentation in the trench is probably controlled more by continental block structure than by the linearity of the trench.

A narrow, continuous pond of sediment partially fills the Central Province trench axis between 32°30'S and 27°S. Trench axis morphology and piston core samples indicate there is transport of terrigenous sediment down the axis from the abundant sediment

supply regions of the Southern Province. A model is formulated from this data which accounts for the sediment wedge in the Central Province by supply of turbidites from the south. A steady-state of axial fill can be maintained by one typical flow every 14 to 27 years.

Uplifted axial turbidites are present on the seaward trench slope at 30°35'S, elevated 350 meters above the axis. Radiocarbon dating puts the age of initial uplift at 5380 ± 350 years B.P., which results in a minimum vertical movement rate of 6.5 cm/yr. Reversed faulting due to compressive stresses generated by plate convergence is the presumed mechanism of uplift.

A model is proposed to explain the differences in the Chilean continental margin morphology in each of the three provinces. The radical differences in the amount of sediment available to the trench axis appears to be a prime influence in the development of the margin. An abundance of axial sediments provides a buffer zone along the major interplate contact (slip) zone, plus material to be accreted into the lower continental slope. If the amount of axial sediments is limited, excessive frictional resistance to slippage between the converging plates may tectonically erode the margin by slowly wearing away the underside of the continental slope.

CHILE TRENCH:
EXTENSIONAL RUPTURE OF OCEANIC CRUST AND THE INFLUENCE OF TECTONICS ON SEDIMENT DISTRIBUTION

by

William John Schweller

A THESIS

submitted to

Oregon State University

in partial fulfillment of
the requirements for the
degree of

Master of Science

June 1976

APPROVED:

Redacted for Privacy

Professor of Oceanography
in charge of major

Redacted for Privacy

Dean of School of Oceanography

Redacted for Privacy

Dean of Graduate School

Date thesis presented on 27 February 1976

Typed by Margie Wolski for William John Schweller

ACKNOWLEDGEMENTS

My primary debt of gratitude is to Dr. L. D. Kulm, not only for his scientific guidance, but for the much more difficult task of allowing me the freedom to wander down my own paths of inquiry, irregardless of how misdirected they must have often seemed. Thanks are also due to Drs. R. Lawrence, S. Johnson, and S. Wilson for serving on my committee.

Stimulating discussions with my fellow graduate students and aid from the indispensible technicians helped get me through the low times. In particular, thanks to R. Prince for unfailing help on land and sea, and to B. Selk, S. Swift, and T. Chriss for technical assistance and enlightening comments.

Drafting above and beyond my puny ability was done by S. Kulm and M. Dibble. Final typing was done by the dexterous digits of M. Wolski.

Finally, my sincerest appreciation to my parents for helping me along the way, and to Charles White for the initial inspiration toward this goal.

Funding for this research was provided by National Science Foundation grant no. IDO 71-04208 under the IDOE Nazca Plate Project.

TABLE OF CONTENTS

LIST OF FIGURES

List of Figures, continued:

LIST OF TABLES

CHILE TRENCH:
EXTENSIONAL RUPTURE OF OCEANIC CRUST AND THE INFLUENCE OF TECTONICS ON SEDIMENT DISTRIBUTION

INTRODUCTION

Deep-sea trenches are essential parts in the puzzle of plate tectonics and play an important role in the evolution of continental margins. These features are not only the deepest areas in the ocean, but are also associated with zones of destructive earthquakes and with huge onshore mineral deposits. Despite this importance, major questions about trenches remain unanswered, particularly concerning the fate of the oceanic lithosphere and its blanket of pelagic and continentally-derived sediments as they are subducted.

The Peru-Chile Trench is a continuous depression some 5000 kilometers long lying along nearly the entire western coast of South America from Ecuador to southern Chile. The segment of trench south of the border between Peru and Chile at 18°S, referred to as the Chile Trench, is anomalous for two main reasons: First, it is one of the few trenches in the world that is linear rather than arc-shaped. Second, although the Andes rise to over 6000 meters above sea level, large parts of the northern trench axis only 250 km distant from these mountains are virtually barren of sediment. In contrast, the southern sections of the trench are nearly buried by axial sediments over a kilometer thick, even though the trench axis is much

shallower in the south. This great variation of sediment cover, which is related to the wide range of onshore climatic conditions, creates a unique opportunity to determine what effects the supply of sediment to the trench axis has on the development of the contiguous continental margin. The paucity of sediment in the northern sections of the Chile Trench also provides excellent visibility of structural disruptions of the oceanic crust as it bends downward into the trench.

The intent of this study is to produce an integrated model of the Chile Trench by combining data on bathymetry and morphology, sediment distribution, structural features, and stresses inferred from a plate tectonic framework. It is hoped that this model will not only aid in explaining the present makeup of the trench system, but will also be of some use as a predictive tool to explain the evolution of a convergent continental margin.

Previous Oceanographic Studies

The Peru-Chile Trench has been known as a major marine physiographic feature for nearly 100 years. Sir John Murray published the first charts showing the deep areas in 1895, based on soundings from submarine telegraph cable surveys done during the 1870's (Thompson and Murray, 1895). Zeigler et al. (1957) produced the first report dealing specifically with the morphology of the trench and also compiled a history of the earlier explorations. Fisher and Raitt

(1962) initiated geophysical studies of the trench, followed by a more detailed investigation by Hayes (1966). Seismic reflection profiles taken during the 1967 DAVIS expedition were used as evidence for questioning the validity of active subduction in the Chile Trench by Scholl et al. (1968, 1970). Seismicity of the trench and its associated Benioff Zone was examined by Stauder (1973).

The lack of previous work in the trench off northern Chile is reflected in the dearth of trackline coverage shown by Mammerickx et al. (1975). Detailed data are limited to a few scattered studies. For example, Lister (1971) used a single high-resolution seismic reflection profile to analyze the area off Valparaiso at 33°S. Arabasz (1971) included reflection profiles of the upper slope between 23°S and 27°S as part of a thesis on the Atacama Fault system of northern Chile. Ocola and Meyer (1973) and Grow and Bowin (1975) produced crustal cross-sections of the trench and continental margin at 23°S based on seismic refraction and gravity data, with thermal and petrologic data included in the latter study.

Sediment types and distributions were described by Zen (1959) and Bandy and Rodolfo (1964). Lack of precise navigation and of a detailed bathymetric map precluded all but generalized findings. Rosato et al. (1975) compiled all available sediment sample data for the Nazca Plate, but discussed only broad regional patterns.

Magnetic anomalies and fracture zones for the Nazca Plate were

initially mapped and described by Herron (1972). Mammerickx et al. (1975) included a revision of these patterns with their recent bathymetric map of the South Pacific.

Intensive study of the Peru Trench, conducted under the auspices of the International Decade of Ocean Exploration (IDOE) Nazca Plate Project, has resulted in a series of papers on the structures and processes of the trench and continental margin of Peru (Kulm et al., 1973; Prince et al., 1974; Prince, 1974; Kulm et al., 1974; Rosato, 1974; Prince and Kulm, 1975; Masias, 1975; Whitsett, 1976). Comparable geophysical and geological surveying has now been done on a large section of the Chile Trench. Although similar in general tectonic setting to the Peru Trench, the Chile Trench offers some different problems for investigation, primarily because of its linearity and range of sediment cover."

Plate Tectonics Framework

Within the paradigm of plate tectonics, the Peru-Chile Trench is a classic case of oceanic-continental plate convergence resulting in underthrusting of the Nazca Plate beneath the South American continent. Convergence along the Chile Trench is almost due east-west at a relatively rapid rate of 10 cm/yr (Minster et al., 1974). Nazca Plate crust is presently generated at the East Pacific Rise from the equator to about 35°S, and along the south Chile Ridge from 35°S to

45°S. Figure 1 identifies the major tectonic elements of the southeast Pacific and outlines the area of this study.

Prior to 9 million years ago, spreading was occurring along a north-northeast trending ridge system now present as the inactive fossil Galapagos Rise (Herron, 1972). Most of the extent of this ridge and some of its associated magnetic anomaly and fracture zone patterns were described by Mammerickx et al. (1975), relying largely on bathymetry. Fracture zones remain poorly known in the region of the plate extending 500 km seaward of the Chile Trench because of a lack of tracklines. Data from farther seaward on the Nazca Plate indicate that older anomalies strike 330° to 340°, while magnetic anomalies adjacent to the trench trend approximately 330° (Hassanzadeh, 1976). Associated fracture zones would intersect the trench at angles of 60° to 70° if they formed normal to the spreading center.

The Chile continental margin is one of the most seismically active segments of the Circum-Pacific earthquake belt. A well-defined seismic zone extends beneath the continent, apparently tracing the path of the descending oceanic slab. The dip of this zone is steepest (~25°) in the north near the Peru-Chile border at 18°S and flattens to a nearly horizontal plane at 40°S. Both Stauder (1973) and Swift and Carr (1974) found north-south segmentation of the seismic zone into a series of tongues that are subducted independently. Stauder (1973) also analyzed focal mechanisms of coastal earthquakes

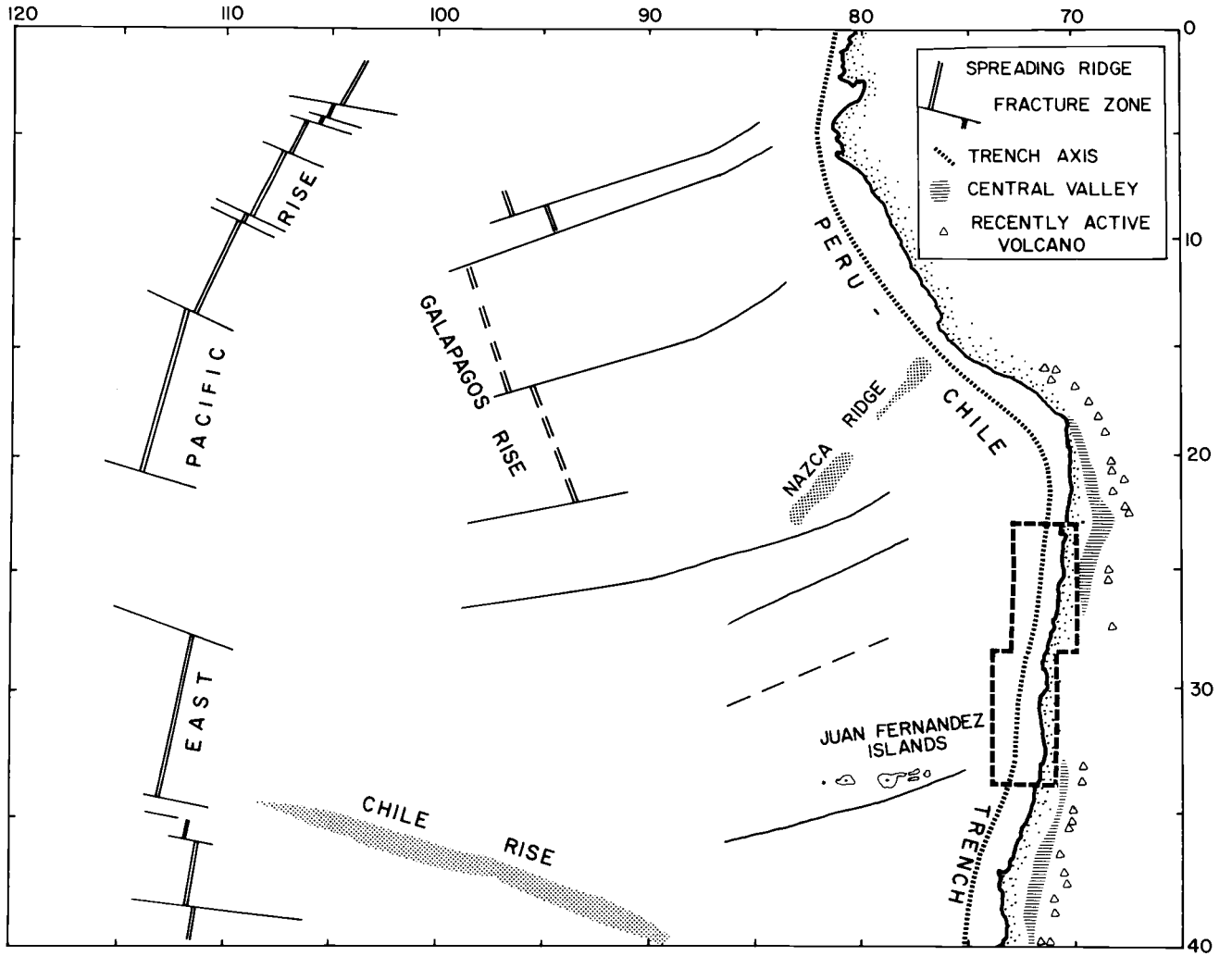

Figure 1. Index map of the Nazca Plate and South American margin. Area of this study outlined by dashed box. Bathymetric and tectonic features from Mammerickx et al. (1975). Active volcanoes and central valley from Casertano (1963).

and concluded that the major seismic activity was due to plate convergence and underthrusting.

Terminology and Vertical Exaggerations

The names applied to important features of the trench and continental margin are shown in Figure 2, and in most cases follow usage in current literature. One departure from common terminology has been made: substitution of "seaward trench slope" for "seaward wall" as a label for the section of oceanic crust between the outer trench slope break and the trench axis. Use of the term "wall" for a feature which has an average slope of only three to four degrees is not only misleading, but creates serious difficulties in visualizing deformational processes.

Similar problems in grasping geometrical relationships are caused by the frequent use of high vertical exaggerations on bathymetric and seismic reflection profiles. Figure 3 shows a single bathymetric profile from the northern section of the study area plotted at several different vertical exaggerations. At 15:1 or more, the V-shape of the trench is emphasized at the expense of hampering recognition of smaller high-relief features within the trench. On the other hand, low exaggerations (2:1 and 1:1) are not only impractically large for display, but make small changes of slope difficult to see. For these reasons, all bathymetric profiles in this study have been

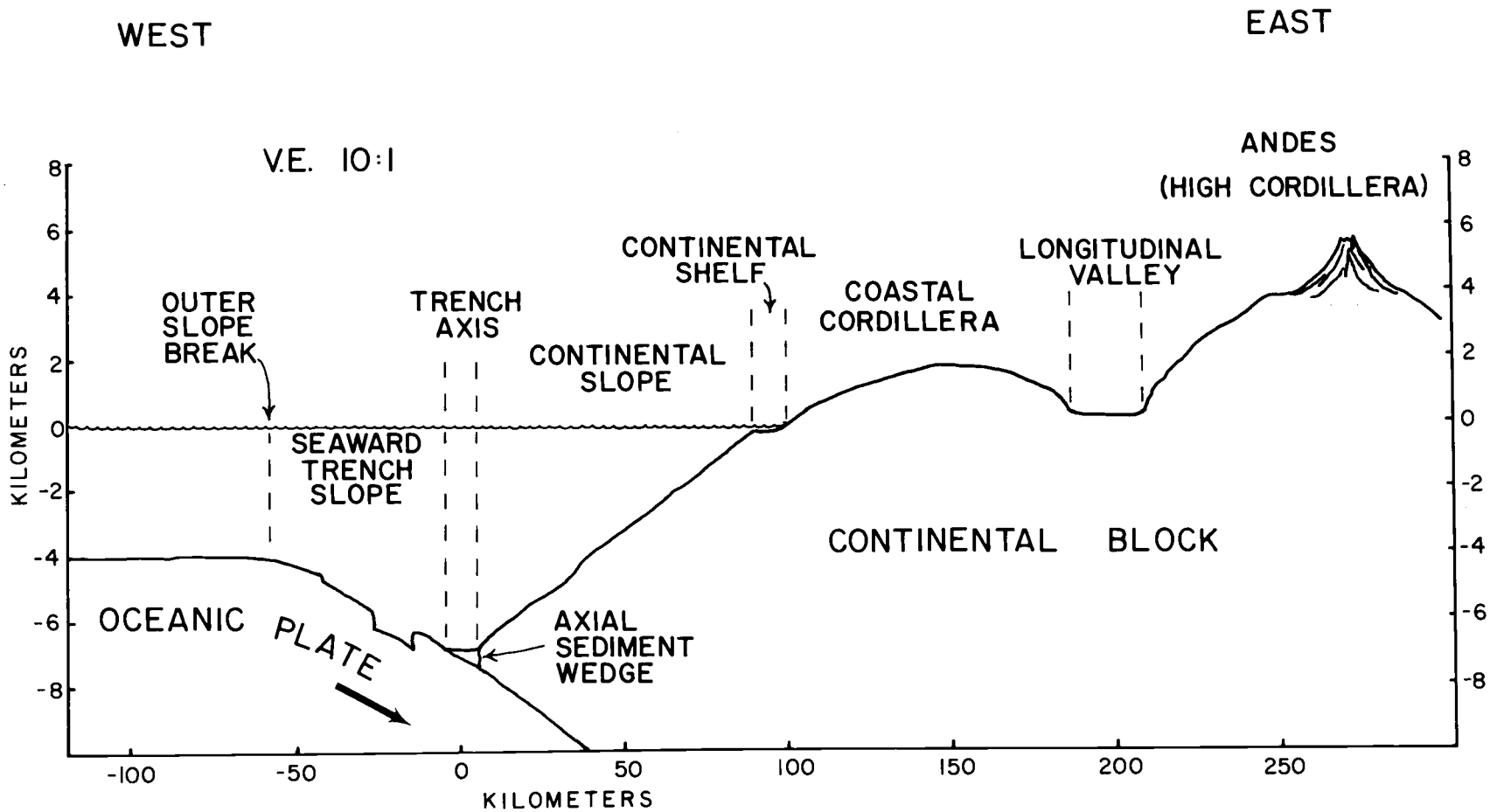

Figure 2. Terminology for major features of the trench and continental margin.

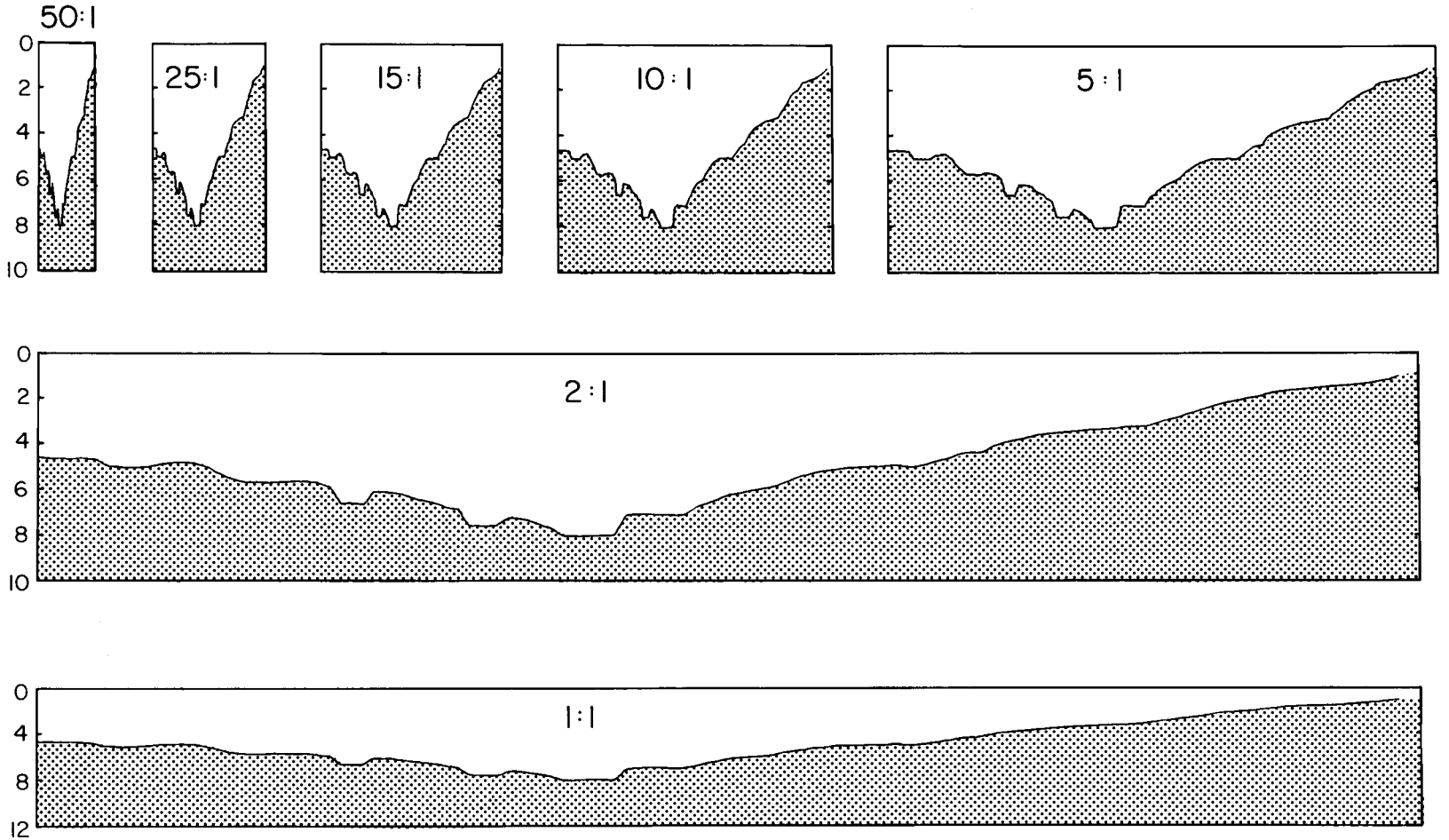

Figure 3. Effect of various vertical exaggerations on a single bathmetric profile. Only the basic shape of the trench is recognizable at 50:1 and 25:1. Benches on the landward slope (right side of axis) are best seen at 15:1 and 10:1, while steep-sided grabens are better defined at 5:1 and 2:1. Profiles at 1:1 (note different vertical scale) are unwieldly and do not show small changes in slope well.

normalized to vertical exaggerations of 10:1, while the seismic reflection profiles are generally at about 5:1. For convenience, all profiles are oriented with east to the right and west to the left.

ONSHORE SETTING

Physiography and geology have a close similarity in northern Chile, since the destruction of outcrops and fault traces in such arid climates is exceedingly slow. The geology of this region has just recently begun to be understood in some detail, due in large part to extensive mapping from aerial photographs. Zeil (1964) presented the most recent compilation of Chilean geology, while other authors (Segerstrom, 1964, 1967; Kausel and Lomnitz, 1968; Arabasz, 1971; Mortimer and Rendic, 1975) have updated coverage of particular areas. The following survey is not intended to be a complete review, but to serve to acquaint the reader with data pertinent to the evolution of the trench and continental margin of Chile. General physiographic features are shown in Figure 1.

Three physiographic provinces are clearly defined in northern and central Chile. From the Peru border at 18°S to approximately the latitude of Copiapo (27°S), a well-defined tripartite profile shows a low Coastal Cordillera, a Central Valley of tectonic origin, and a High Cordillera or Andes with numerous recent volcanic peaks. Between Copiapo and Valparaiso (33°S), the Central or Longitudinal Valley ceases to exist, so that mountains extend unbroken from the Pacific shoreline to the Andes. Transverse east-west valleys characterize this middle zone, along with an absence of recently

active volcanoes along the crest of the Andes. South of Valparaiso, the continental margin once again assumes a profile similar to the northern section, with a coast range, Central Valley and high Andes with numerous historically active volcanoes.

The Coastal Cordillera is a mature range with summit elevations of 1000 to 3000 meters. This range becomes progressively narrower to the north, eventually disappearing to the vicinity of Arica (18°S). Basement units are Precambrian or lower Paleozoic folded metamorphic rocks which have been locally consumed by the intrusion of the Andean batholith complex, particularly in the south. Development of the coastal range is predominantly by block faulting which commenced in the Oligocene and has continued through the present (Kausel and Lomnitz, 1968; Arabasz, 1971). The western edge of this range is typically a wave-cut cliff rising up to several hundred meters above the Pacific shoreline. Marine terraces are well developed along the west-facing slopes south of 27°S, but they are nearly absent to the north with only local benches evidencing changes of relative sea level.

The Longitudinal Valley is a tectonic depression bounded by steep faults on both sides in the section south of 33°S, while north of 27°S it is defined by a western fault against the Coast Range and a monoclinal flexure on the eastern flank rising to the Andes (Kausel and Lomnitz, 1968). Most of the tectonic development took place during the Pliocene, with minor movements still occurring (Muñoz,

1956). Where present, this trough effectively traps virtually all run-off from the Pacific-facing drainage of the Andes. Several kilometers of late Tertiary and Recent alluvial gravels blanket the valley floor in places such as near Santiago (33°S). Following a slightly oblique trend, the Valley intersects the coast at approximately 18°S.

Although the High Cordillera is a continuous topographic feature, it is not homogenous in structure or origin. Very generally, it is a plutonic range consisting of a high plateau or Puna elevated 3000 to 4000 meters above sea level, topped by several hundred andesitic volcanoes rising to maximum heights of nearly 7000 meters. Post-Triassic folding of sediments from two older geosynclinal systems has contributed somewhat to the structures of this range. For many years it was believed that the Andean batholith was emplaced during the Cretaceous. However, recent radiometric dating of the plutonic and volcanic rocks by Farrar et al. (1970) and McNutt et al. (1975) has demonstrated a progressive eastward migration of the axis of intrusive activity since the lower Jurassic. The oldest plutonic rocks are exposed in the Coast Range, while the youngest rocks and the currently active volcanoes are found nearly 200 kilometers to the east. James (1971) speculates among four factors which might produce such a trend, including progressive depression of isotherms and eastward migration of the subduction zone.

DATA COLLECTION AND PROCESSING

Extensive data coverage from recent cruises of the R/V YAQUINA of OSU in 1974, the R/V MELVILLE of the Scripps Institute of Oceanography (SIO) in 1975, and the R/V OCEANOGRAPHER of the Pacific Oceanographic Laboratories in 1973 form the data base in the study area. All new data was collected and processed by OSU personnel except the OCEANOGRAPHER tracklines and profiles. Older data from various cruises was generously provided by Tom Chase of SIO and Bruce Grant of the National Geophysical and Solar-Terrestrial Data Center.

Bathymetric soundings and shallow sediment reflection data were obtained using 12 KHz and 3.5 KHz sources and standard graphic recorders. Deeper penetration seismic reflection records were taken on the 1974 YAQUINA cruise using single or paired airguns ranging from 40 in^3 to 140 in^3. The receiver system consisted of single channel hydrophone streamers, amplifiers, and graphic recorders with a four second sweep rate. Band pass filter settings were generally set at 30 to 100 Hz.

Navigation for the 1973-75 cruises listed above was by earth-orbiting satellite. Data from older non-satellite navigated cruises was used in areas where better data coverage was lacking. Bathymetry was digitized and computer processed to convert to corrected

meters using the Matthews Tables for zones 42 and 43.

A new bathymetric map has been prepared (Figure 4), giving priority to tracklines navigated by satellite (Figure 5). The 200 meter contour interval was chosen as the finest detail that could be reliably correlated between most adjacent tracklines.

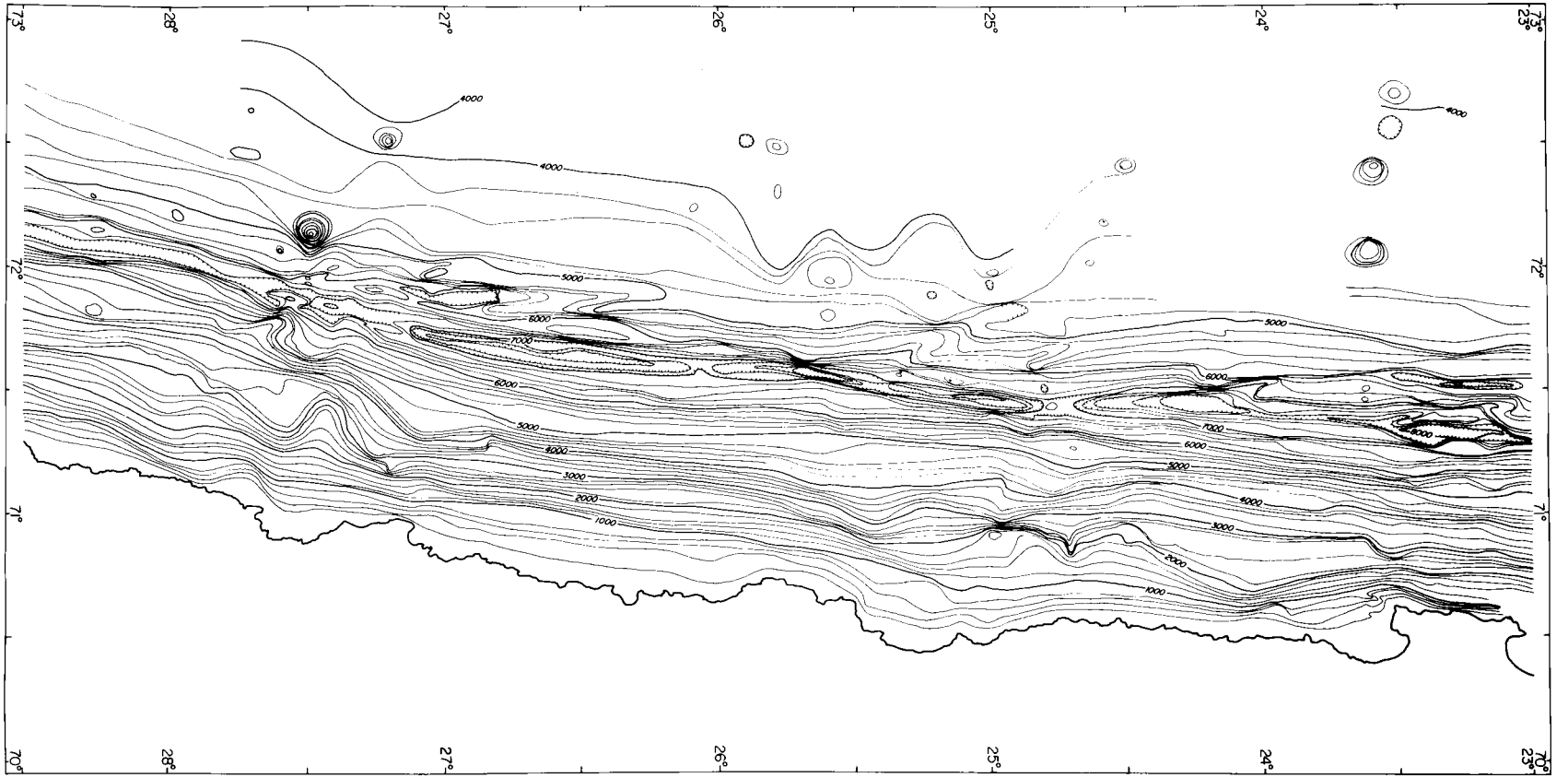

Figure 4. Bathymetric map of the Chile Trench; northern section. Depths in corrected meters, contour interval 200 meters.

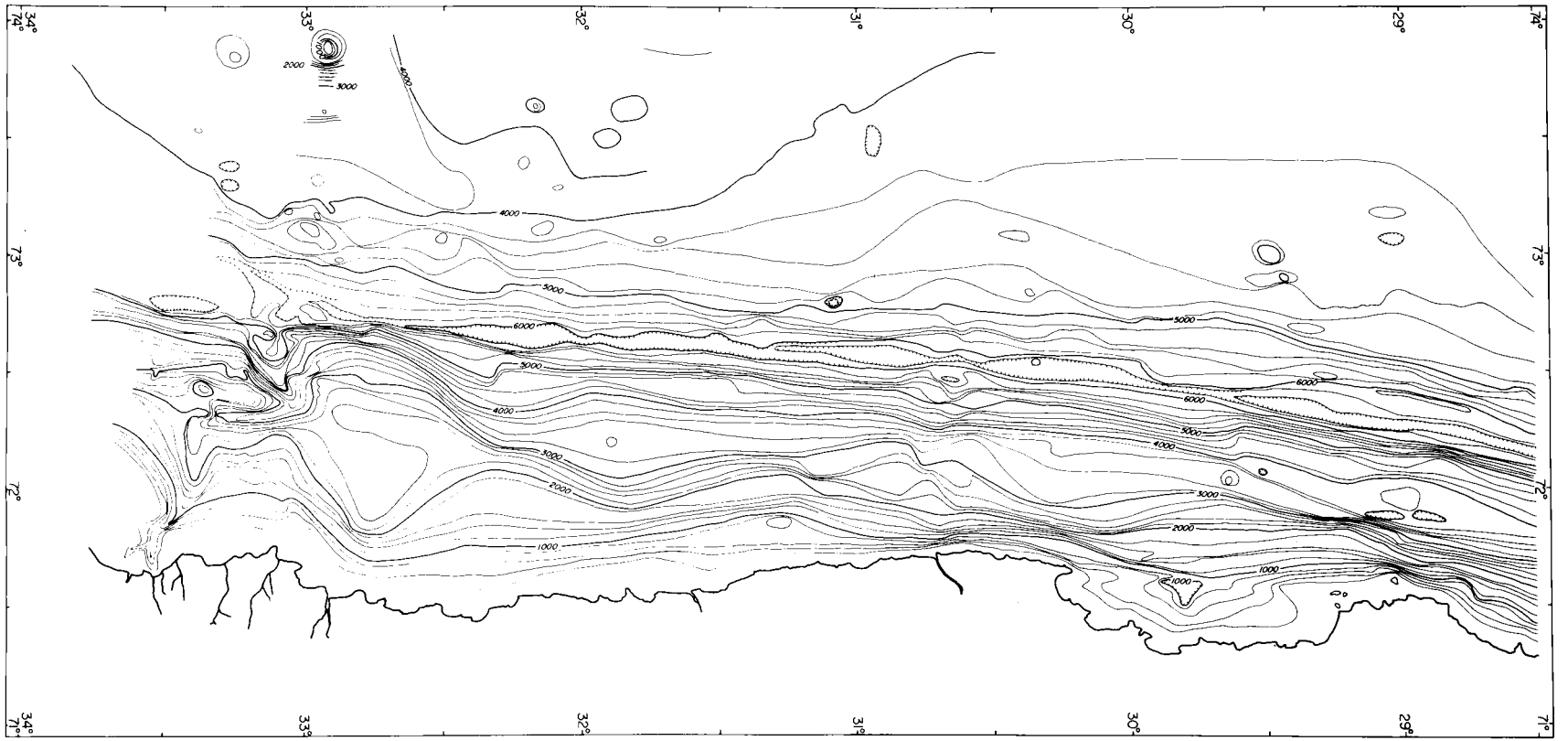

Figure 4 (cont.). Bathymetric map of the Chile Trench; southern section.

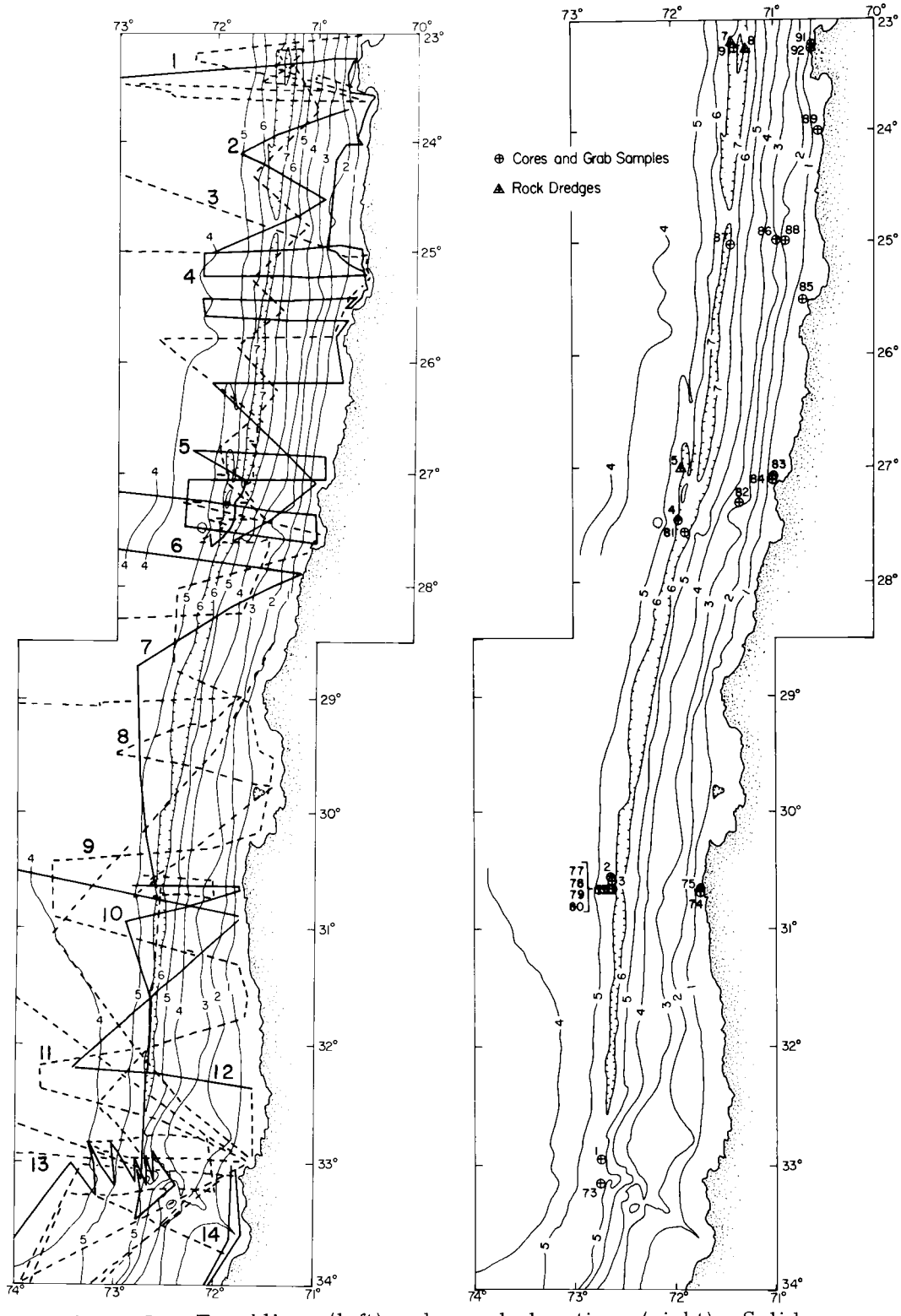

Figure 5. Tracklines (left) and sample locations (right). Solid tracklines are seismic reflection profiles; dashed lines are bathymetry only. Numbered tracklines refer to profiles on Figure 11.

GEOLOGIC SAMPLES

Eighteen rock or sediment samples were taken from the trench area during the 1974-75 cruises using a variety of sampling equipment, mainly rock dredges and piston cores. In addition, nine nearshore sites in water depths as deep as 400 meters were sampled in conjunction with Chilean mineral exploration and sediment studies. These sample sites are shown on Figure 5, while Appendix 1 lists the location, depth, and a brief description of each sample.

Trench axis cores (1, 73, 78, 79) consist predominantly of turbidites whose basal units are medium to fine sand with high mica and mafic mineral content. In only one core (3), discussed in a latter section of this study, are these turbidites significantly displaced above the trench axis. Hemipelagic muds dominate the remainder of the trench sediments on both sides of the axis, showing general mottling but no other internal structures (4, 9, 77). Some nearshore and upper slope areas seem to be nearly barren of soft sediments. Repeated attempts to sample with various grabs and corers yielded only sparse returns of sand or hard clays (84, 88, 91, 92).

Rock dredges across steep scarps on the seaward trench slope near the trench axis returned oceanic pillow basalts, massive basalts, and small amounts of volcanic breccia (5, 7). Attempts to

dredge a steep scarp at the base of the continental slope yielded a large amount of loosely consolidated muds and sands with a small proportion of well-cemented sandstones of similar materials (8).

PROVINCES AND FEATURES OF THE TRENCH

The Chile Trench shows an enormous variety of structures over the area of this study. Any attempt to portray the entire trench as a single structural unit is thus destined either to overgeneralize and ignore the variations, or to particularize all of the variations and confound the general trends which do exist. Fortunately, there are zones which maintain similar morphologic and structural traits over sizable areas, separated by distinct, abrupt transitions. These transitions occur at the same latitudes in the trench axis as on the seaward trench slope, and to a lesser degree on the continental slope. Thus the definition of trench provinces is a fairly straightforward task and has been done on a gross scale by both Hayes (1966) and Scholl et al. (1970). New data presented in this study allow refinements of these divisions and a more detailed analysis of the characteristics of each province. The following sections progress in a north to south sequence.

Northern Province

The northern province of the Chile Trench consists of a series of isolated axial basins, each with a small pond of horizontally layered sediments, separated by shoaler areas or saddles in the axis which rise up to 500 meters above the level of the adjacent

basins (Figure 6). Five such basins lie in the axis between 23°S to 27°S (Figure 7), becoming successively deeper to the north. The maximum depth in the trench is attained on the northernmost basin near 23°20'S, reaching 8065 meters. Although the general saddle and basin character of this province seems to continue north of 23°S (Coulbourn and Moberly, 1976), the axial depths diminish slightly, marking the 23°S basin as the deepest sounding in the eastern Pacific Ocean.

A seismic reflection profiles across this basin at 23°15'S (Figure 8) shows flat reflecting horizons, inferred to be turbidite deposits, in the trench axis overlying the oceanic plate acoustic basement which dips to the east beneath the continental slope at point A. (The pelagic sediment cover on the incoming plate is too thin to be resolved acoustically.) The 5 km-wide sediment pond is wedge-shaped with maximum thickness of 0.4 seconds (two-way travel time, or about 350 meters assuming a velocity of 1.7 km/sec) against the base of the continental slope. While most of the isolated basins are not as large as this one, the general forms are homologous.

The morphology of the seaward trench slope appears to be controlled by large-scale block faulting which produces a much higher relief than is normally found on the Nazca Plate to the west. Major features strongly resemble horst and graben structures and trend subparallel to the trench axis for distances up to 100 km. The major fault traces, shown in Figure 7, have vertical offsets of 500 to 1000

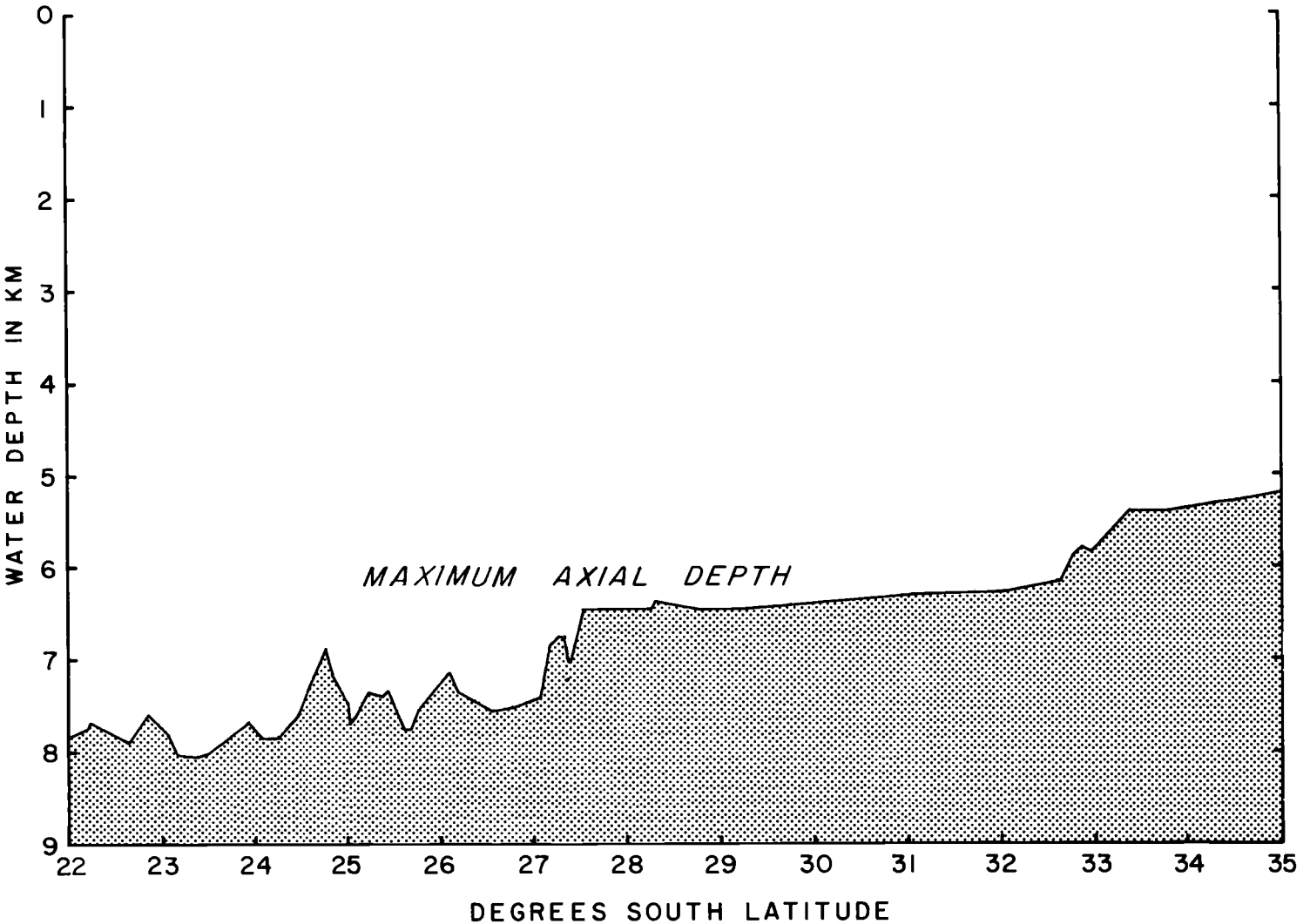

Figure 6. Longitudinal profile along the axis of the Chile Trench.

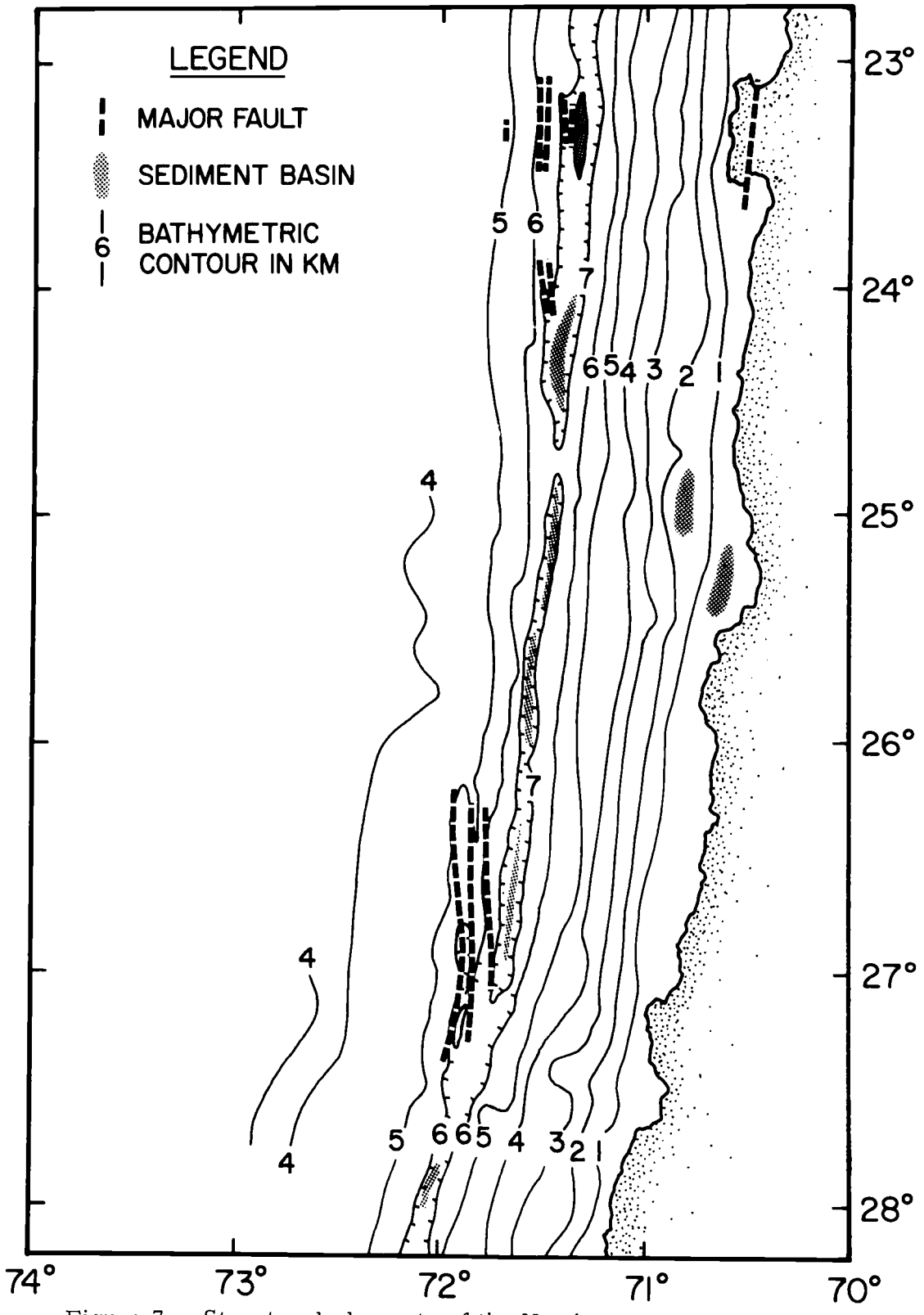

Figure 7. Structural elements of the Northern Province of the Chile Trench.

meters. Dips on these scarps exceed the 30° limit of resolution for shipboard acoustic systems, while the acoustic-basement surface of the faulted blocks retains the general slope of the adjacent oceanic plate. Faulting is evident from the trench axis up to the vicinity of the outer trench slope break (Figure 8, A to D). The magnitude of offset increases sharply as the plate begins to curve downward, reaching its maximum extent by approximately the 5000 meter contour with minimal additional offset developing below this depth. Figure 8 shows development of fault blocks at 23°S, including incipient faulting just below the outer trench slope break (D), while Figure 9 shows a single graben at 27°S.

Sediment cover on the seaward trench slope is relatively thin, in most places amounting to less than 100 meters. One exception to this general distribution exists on the floor of a graben 700 meters above and over six kilometers west of the trench axis at 23°15'S (Figure 8, point B). Horizontal layering of sediments in this wedge-shaped deposit indicates deposition after the oceanic plate began its descent into the axis. A piston core (9) recovered normal hemipelagic muds, perhaps derived by slumping of existing sediments from the oversteepened edges of the faulted blocks on either side of this basin.

In contrast, the continental slope in this province has a remarkably constant gradient and lacks topographic evidence of major deformation. There is a general absence of benches and block

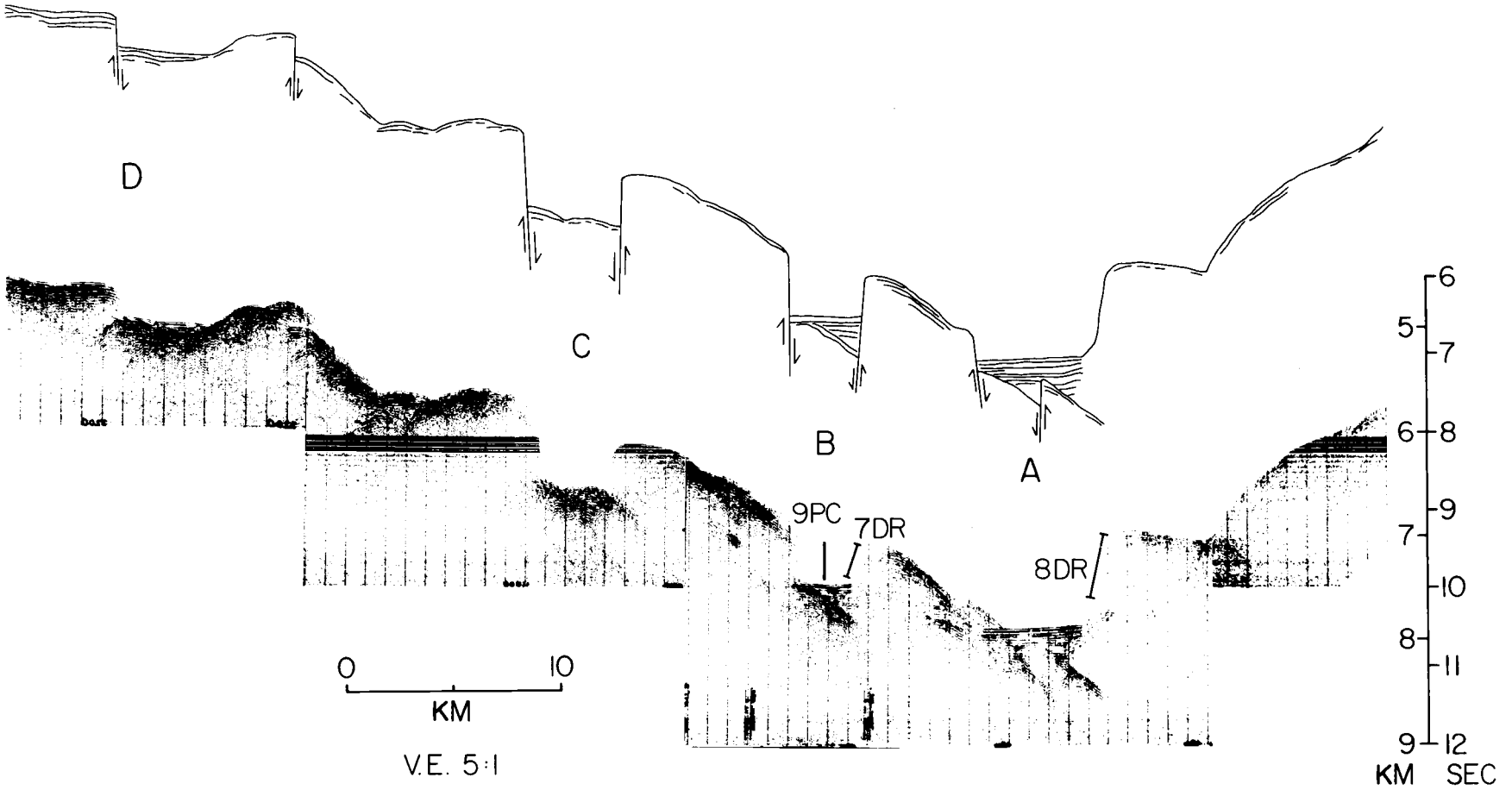

Figure 8. Seismic reflection profile at 23°15'S, showing faulting beneath undisturbed turbidites in the axis (A), grabens on the seaward trench slope (B, C), and incipient normal faulting near the trench slope break (D).

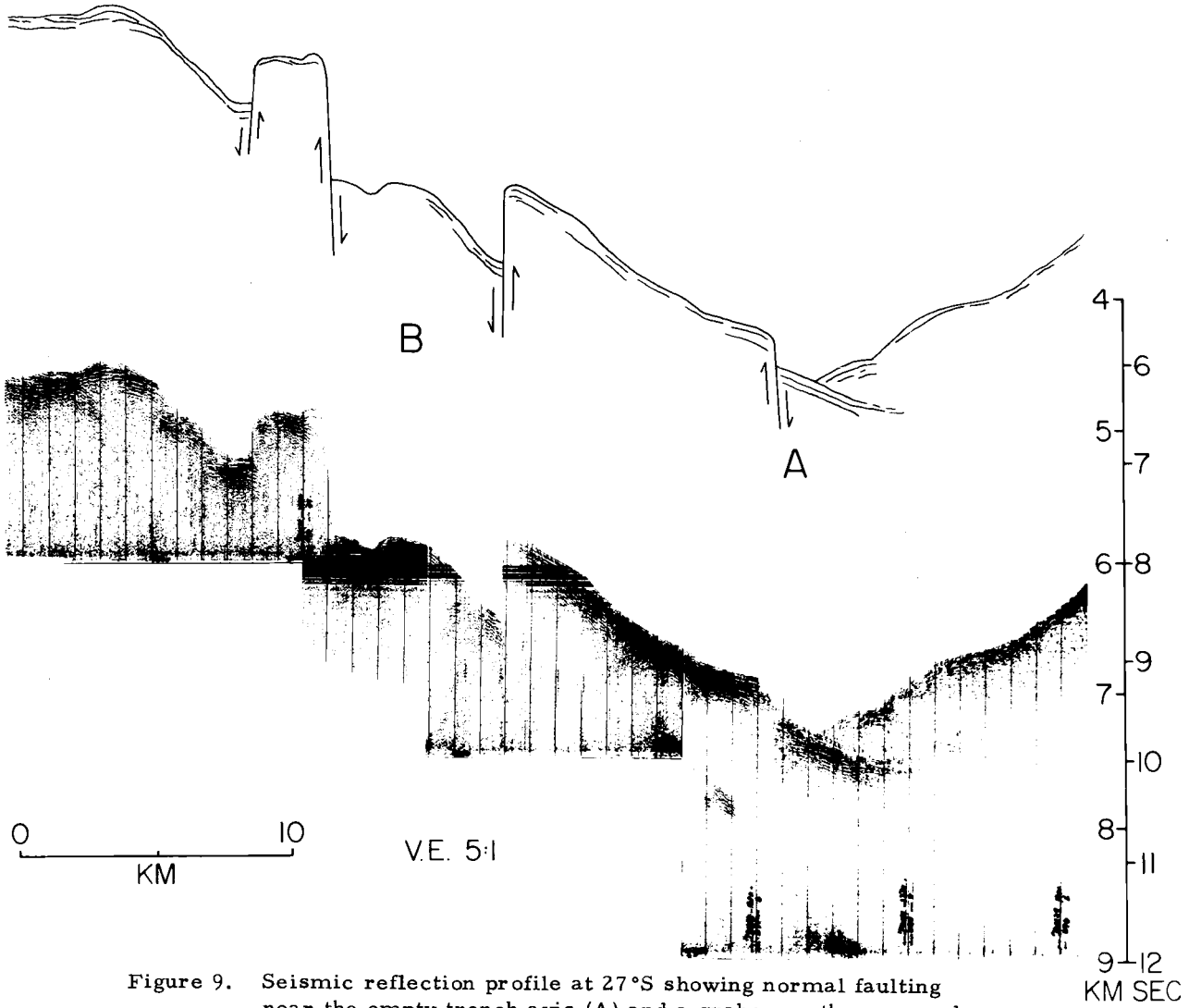

Figure 9. Seismic reflection profile at 27°S showing normal faulting near the empty trench axis (A) and a graben on the seaward trench slope (B).

faulted features common to the continental slope in the Peru Trench (Prince, 1974). Upper slope basins are small and poorly defined on reflection records. Except for a thin hemipelagic cover, the sediments and rock outcrops of the middle and lower slope are acoustically unresolvable. Arabasz (1971) reported evidence for block faulting on the upper slope between 23°S and 27°S. Seismic reflection from the 1974 cruise indicates that this faulting is limited to minor offsets in the upper slope, particularly within the layered sediments, and is not commonly present on the middle or lower continental slope.

The continental shelf is almost absent along most of the coast, with the 200 meter contour only 2 to 8 km offshore. In the few instances where tracklines approach the shore closely enough, the shelf break occurs at 110 to 150 meters. This narrowness of the shelf is not surprising in view of the steep upper continental slope and the precipitous coastal morphology.

The presence of turbidites in the isolated basins in the trench axis poses a perplexing situation. Fluvial sediment input to this area is negligible because of the extremely arid climate and the lack of continental drainage patterns leading to the shore. The absence of submarine canyons or an appreciable sediment cover on the continental slope argues strongly against large volume downslope transport of material from the adjacent coast. Transport via turbidity flows progressing down the axis from the sediment-rich provinces to the

to the south is a more attractive alternative from the standpoint of availability of source materials. However, there is no visible sediment in seismic reflection records across the saddles that separate the axial basins (Figure 9). Since it is unlikely that turbidity flows with appreciable fine to coarse sand would be able to flow over the relief now present along the trench axis (200 to 500 m), these turbidites would then have to predate the uplift of the saddles.

At least three possible origins for the isolated turbidite ponds can be formulated from the available data: (1) deposition by axial turbidity flows from the south, followed by uplift of the saddle areas and erosion of the deposits from the saddles by bottom currents; (2) deposition and subsequent uplift as in (1), but with deformation associated with uplift making the turbidites on the saddles acoustically unresolvable, and (3) downslope transport into pre-existing structural depressions by turbidity flows generated on the adjacent narrow continental shelf during the last glacial period, when sea level was lower and when increased rainfall would provide a slightly larger number of sources and/or a larger volume of sediment. No subsequent deformation is required in this last case if the depressions existed along the trench axis prior to deposition of the turbidites. None of these hypotheses are particularly satisfying, but a more complete explanation must await further sampling and dating of these isolated basin deposits.

Central Province

Four features define the transition zone between the northern and central provinces at 27°00' to 27°30'S. The most obvious of these is a sharp decrease in axial depth of 1000 meters within one-half degree latitude (Figure 6). Large horst and graben structures on the seaward trench slope disappear abruptly just south of 27°S, while benches are seen for the first time on the continental slope and extend southward. Lastly, the trend of the trench axis changes from N 5° E (Northern Province) to N 20° E (Central Province) between 27°00'S and 27°15'S. The simultaneous occurrence of these four features suggests that a major structural break exists near 27°S in the trench.

A continuous but narrow pond of sediment partially fills the trench axis along the Central Province, maintaining an extraordinarily uniform depth of about 6400 meters with a very gentle gradient of 1:2000 upslope to the south along a distance of over 500 km. This sediment level is controlled in part by an acoustic basement block in the axis centered around 27°15'S. Width and thickness of the sediment wedge are variable, indicating that the sediment covers considerable basement relief. Sediment thicknesses of up to 0.4 seconds (350 m) occur in the trench, but the average along the province is much less, on the order of 0.1 to 0.2 seconds (85 to 175 m).

None of the large block-fault features dominant in the Northern Province are visible on the seaward trench slope between 27°S and 33°S. However, some faulting is visible beneath the ponded sediments in the axis both in this province and further to the south. Figure 10 shows a ridge of acoustic basement rising to just above the surface of the axial turbidites at 31°S. This feature is inferred to be a faulted block of oceanic crust, although its form is not as well defined as those to the north. Most of the fault offset developed before the feature entered the area of turbidite deposition, since the axial sediments are still horizontally layered. Sparcity of seismic reflection profiles in the central province precludes a more detailed examination of these buried fault blocks.

The continental slope is less steep along this section than to the north, although the shoreline-axis width remains the same (95 ± 10 km). Shallower axial depths reduce the overall slope gradient to 1:15, or about 4°. The continental slope in this province is interrupted by a major bench extending nearly the entire length of the province (Figure 11). Starting at less than 3000 meters near 32°S, this bench gradually slants down the slope to the north, reaching a maximum depth of 5000 meters at its northern end at 28°S. The bench is about 500 km long and varies irregularly in width from 15 to 40 km. No structures or sediments are discernable beneath the irregular surface of the bench, indicating that it is not a simple

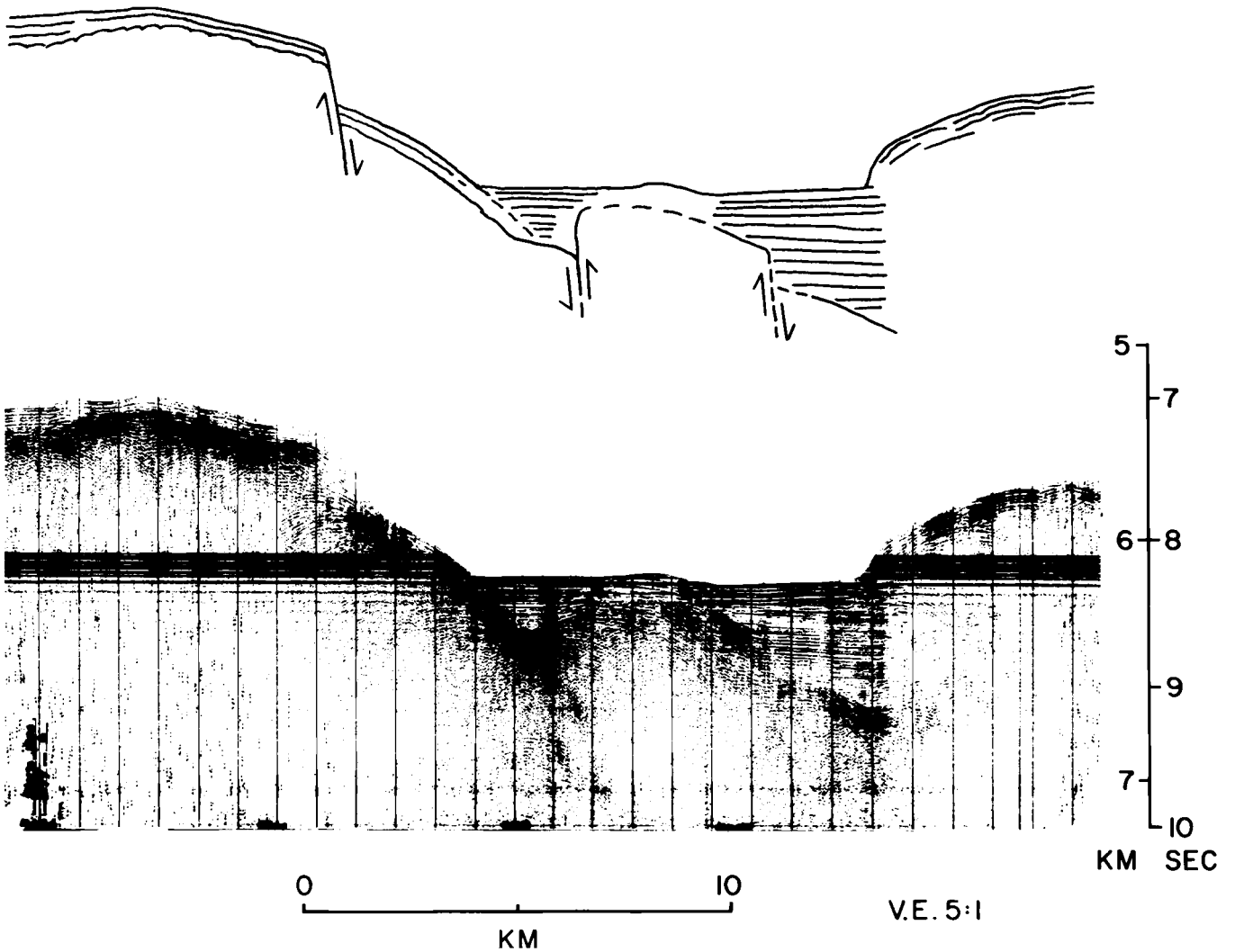

Figure 10. Seismic reflection profile at 31°S showing ponded axial sediments in the Central Province.

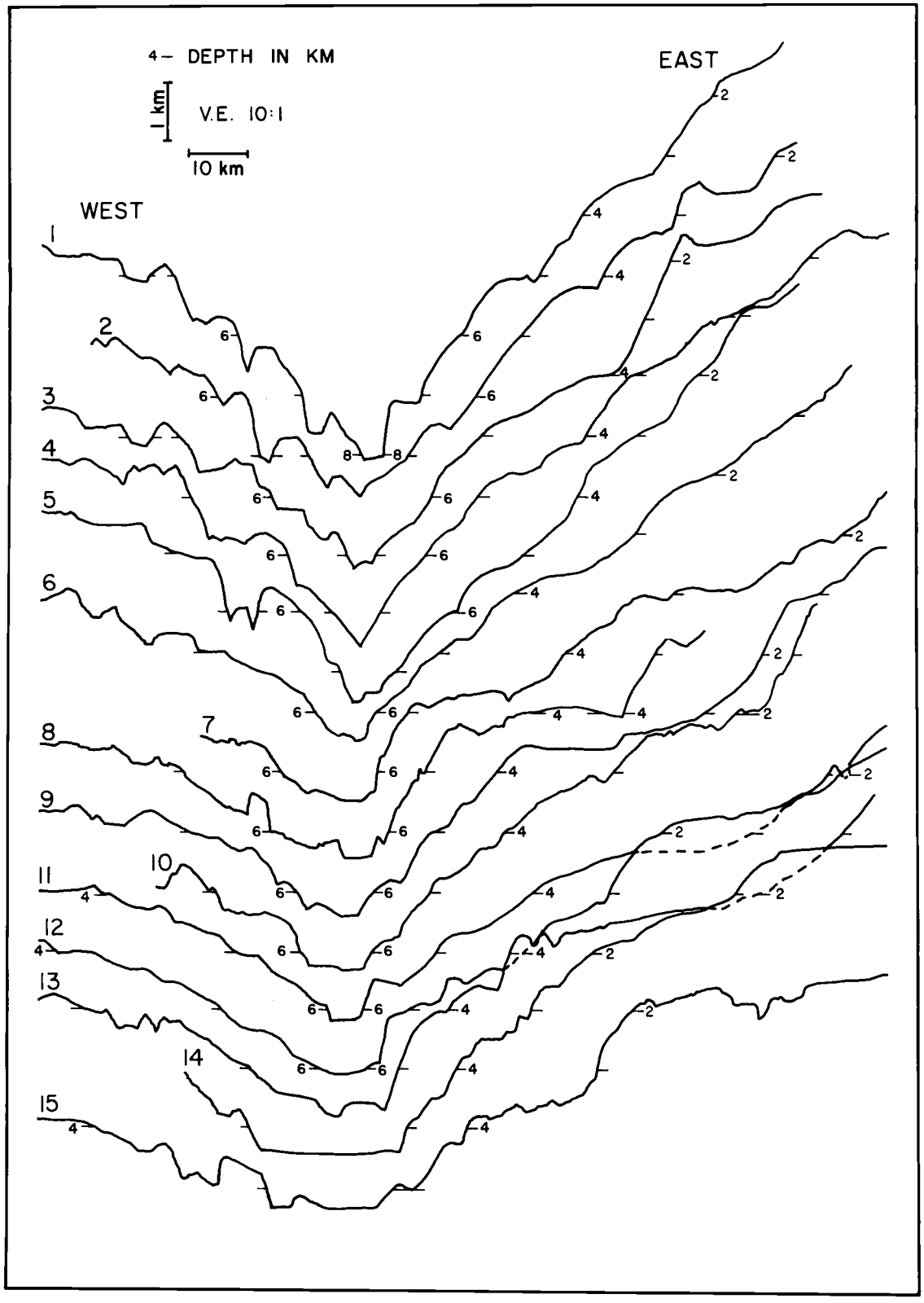

Figure 11. Bathymetric profiles across the Chile Trench, 23°S to 34°S. See Figure 5 for locations.

sediment basin as are the trench axis ponds and upper slope basins in the Northern Province.

Uplifted Turbidites

Turbidites occur 350 meters above the trench axis on the seaward trench slope eight kilometers west of the axis near 30°35'S (Figure 12). A piston core (FD-75-3 PC) taken on a bench at 30°34'S, 72°38'W sampled three thin sand turbidites within a 60 cm section of hemipelagic sediment, with nearly seven meters of homogenous hemipelagic clays comprising the lower sections of the core. The sands are highly micaceous, fine to medium grained, and contain numerous fine fragments of leaves and other vegetal debris. The presence of similar material in a much thicker sand turbidite sequence at 33°S and absence of a proximal source area for these sands north of 33°S suggest longitudinal transport of sediments down the trench axis from south to north by turbidity currents.

Deposition of these sand turbidites in their present position would require upslope transport of ten times the maximum elevation documented by Bennets and Pilkey (in press) for turbidites with retention of the sand fraction of the sediment load. A more likely alternative is that tectonic uplift occurred at this site relative to the trench axis shortly after the descending plate encountered the trench axis turbidite regime. The uniform regional gradient of the

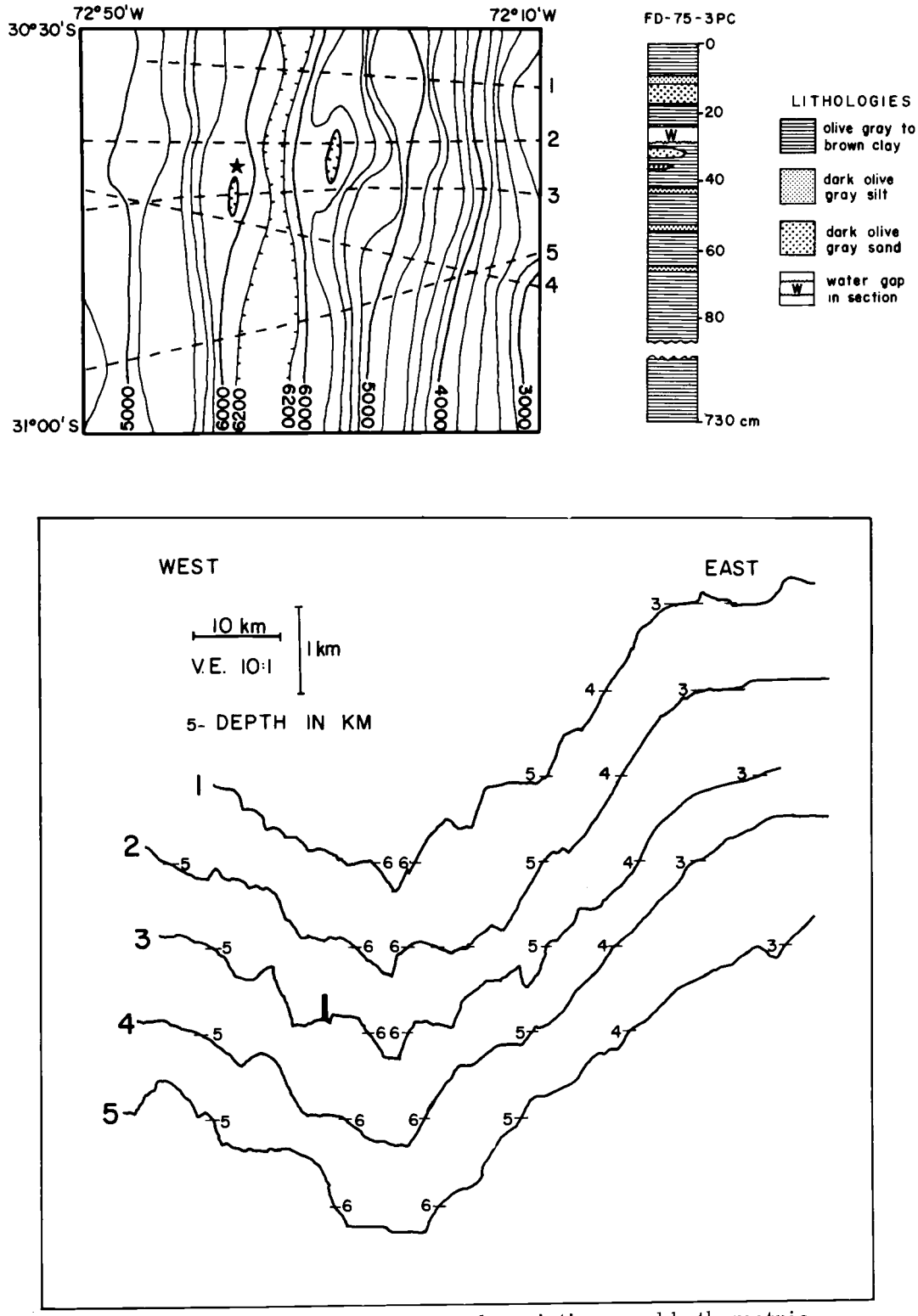

Figure 12. Core location, core description, and bathymetric profiles for the uplifted turbidites at 30°35'S.

axis (Figure 6) indicates that absolute uplift of a limited section of oceanic crust on the seaward trench slope is more reasonable than a drop in the trench axis depth in the vicinity of this site.

Radiocarbon dating of the upper sand turbidite from this site at 31°S yields an age of 5380 ± 350 years. Since that date, uplift of 350 meters has occurred relative to the trench axis, but there is no way of determining over what portion of this time uplift has been active. A similar case has been reported by Prince et al. (1974) for a site in the Peru Trench at 8°S, with uplift of 700 meters in 5100 years. Rapid, large-scale vertical tectonic activity in the vicinity of trench axes may be more common than previously suspected.

Southern Province

At approximately 32°30'S, the trench again undergoes a radical change of form in conjunction with an abrupt step in trench depth (Figure 6). An abrupt increase in axial sediment fill is the major difference between the Central and Southern Provinces, altering the shape of the trench axis from a narrow trough to a wide, flat floored depression (Figure 13). Proximity of the major seaport of Valparaiso at 33°S has resulted in an abundance of generally east-west oriented tracklines which parallel the complex transition zone located between 32°45'S and 33°15'S. An additional set of seismic reflection lines was run normal to this orientation to provide three-dimensional

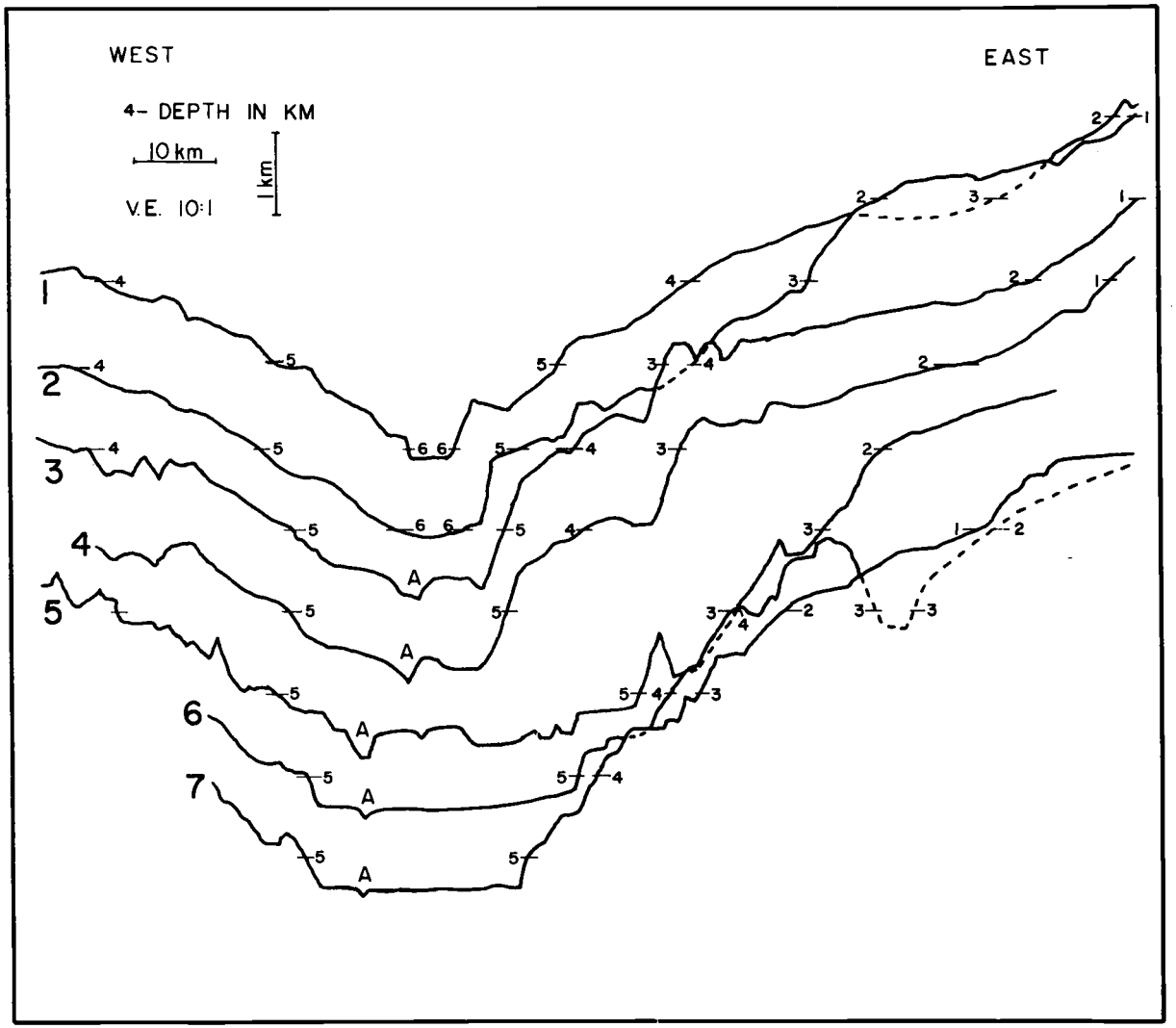

Figure 13. Bathymetric profiles across the trench axis between 32° 00' and 33° 40' showing the transition from sediment filled axis to nearly empty axis. Point A is a deep-sea channel discussed in the text. See Figure 15 for profile locations.

structural control (Figure 5). To aid in visualizing this zone, a single-point perspective drawing (Figure 14) was constructed from the bathymetry (Figure 15), showing the area as it would appear looking eastward across the axis from a viewpoint over the Pacific Ocean.

From 33°S to at least 40°S, the trench axis, as a bathymetric feature, is nearly obscured by a kilometer or more of horizontally layered sediments, inferred to be turbidites. Large block fault features similar to those in the northern province can be seen on the gently dipping seaward trench slope and within the trench axis beneath these sediments (Figure 16). As in the north, development of the fault offsets takes place mainly on the seaward slope, since the ponded sediments maintain their horizontal layering around the buried blocks in the trench axis.

A deep-sea channel occurs in these axial sediments, extending along the seaward edge of the filled axis downslope to the north (Figure 15). Nearing 33°S, the channel form becomes a V-notch, cutting deeper into the turbidites in response to a steepened axial gradient (Figure 6). This erosional channel, recognized by Lister (1971), gradually widens into the narrow, deeper axis to the north and loses its channel character by 32°45'S. The development of channel morphology in response to structural control and the gradient of the axis can be traced in Figure 13, and dominates the foreground of the perspective view (Figure 14).

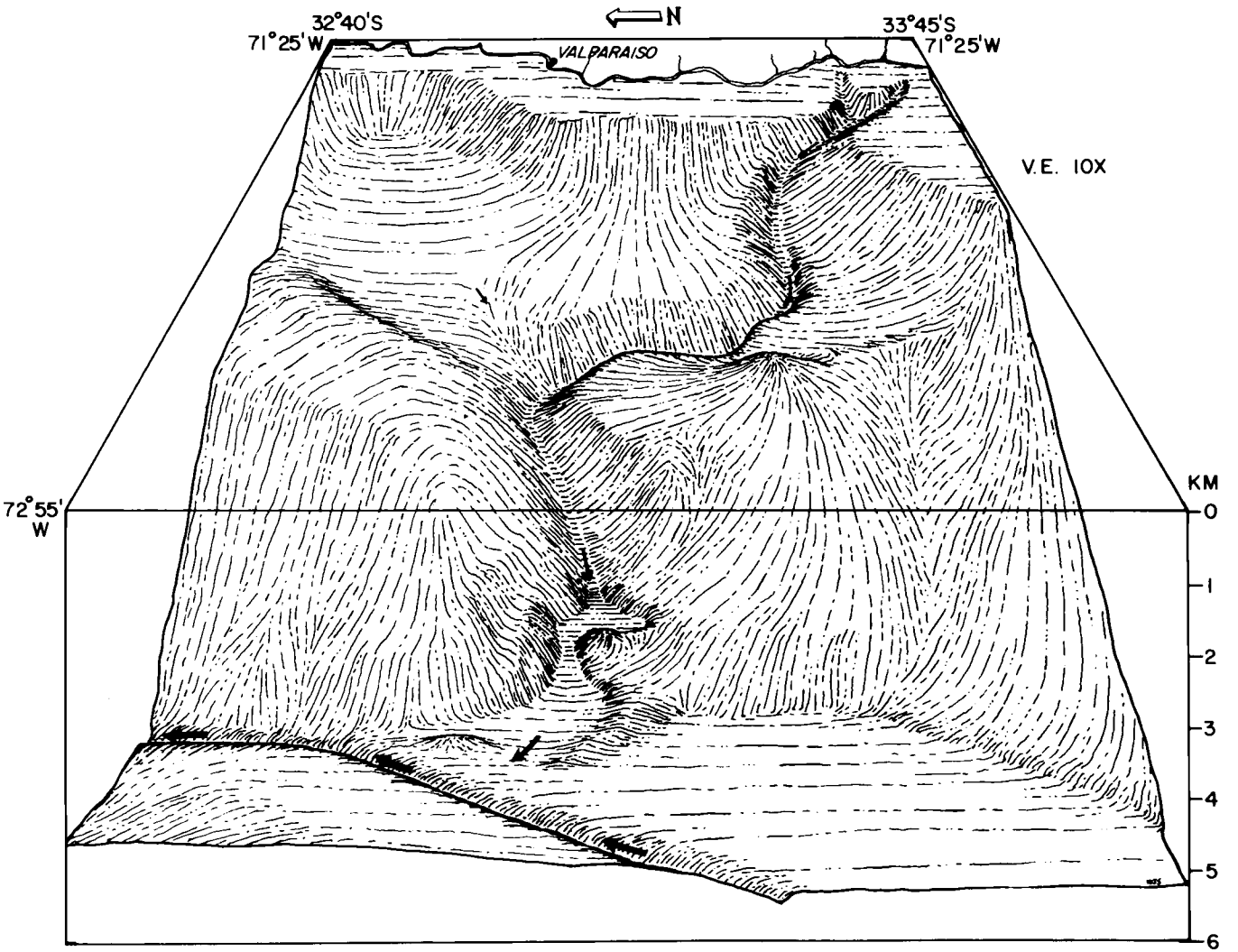

Figure 14. Single point perspective drawing of the trench axis and continental slope at 33° S, based on bathymetry of Figure 4. Location of area shown is outlined on Figure 15. Arrows represent downslope sediment transport vectors.

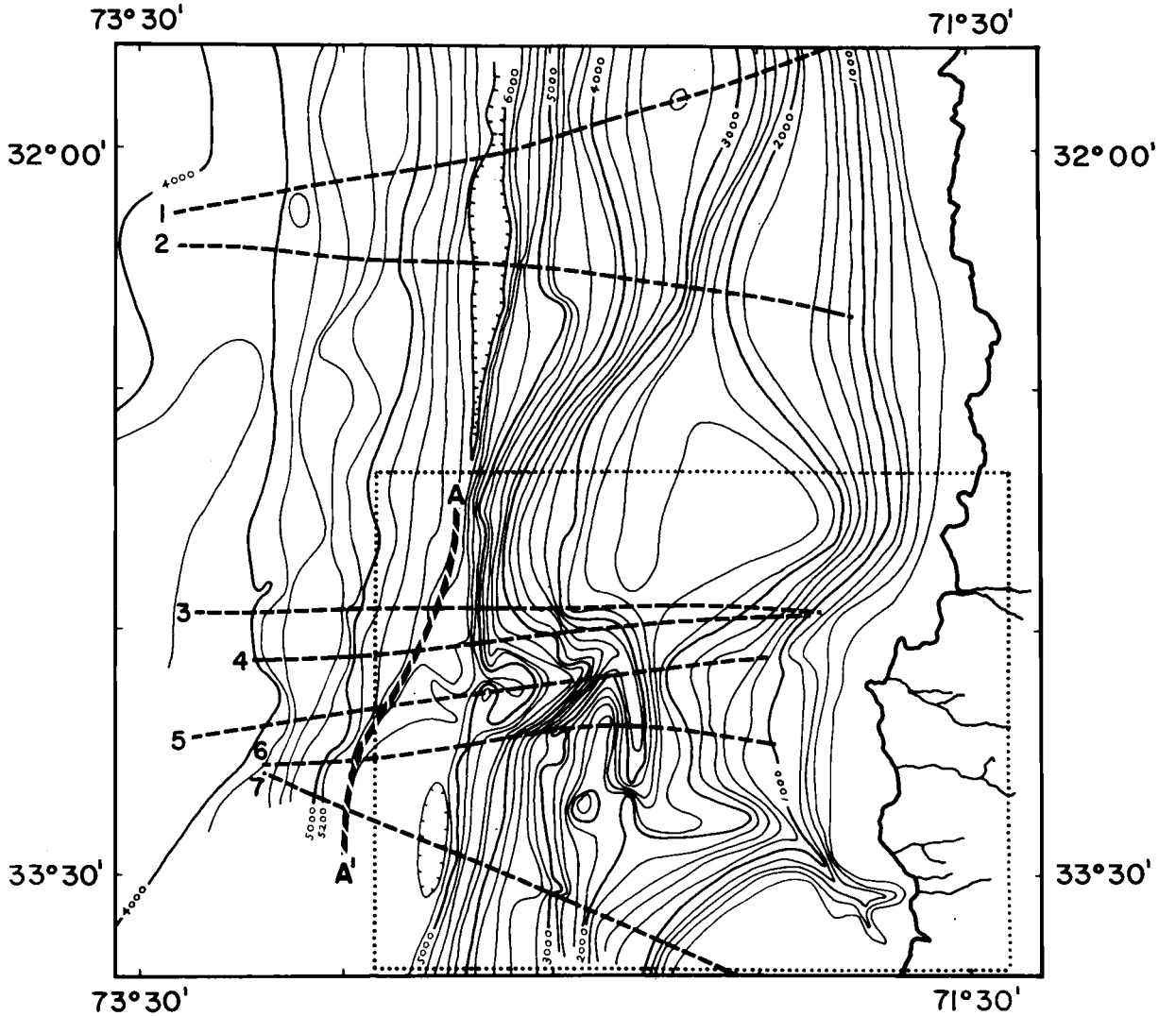

Figure 15. Detail map of 33° S transition zone. Area of the perspective view (Figure 14) is outlined by the dotted line box. Numbered dashed lines refer to bathymetric profiles of Figure 13. Line A - A' is a deep-sea channel in the axis.

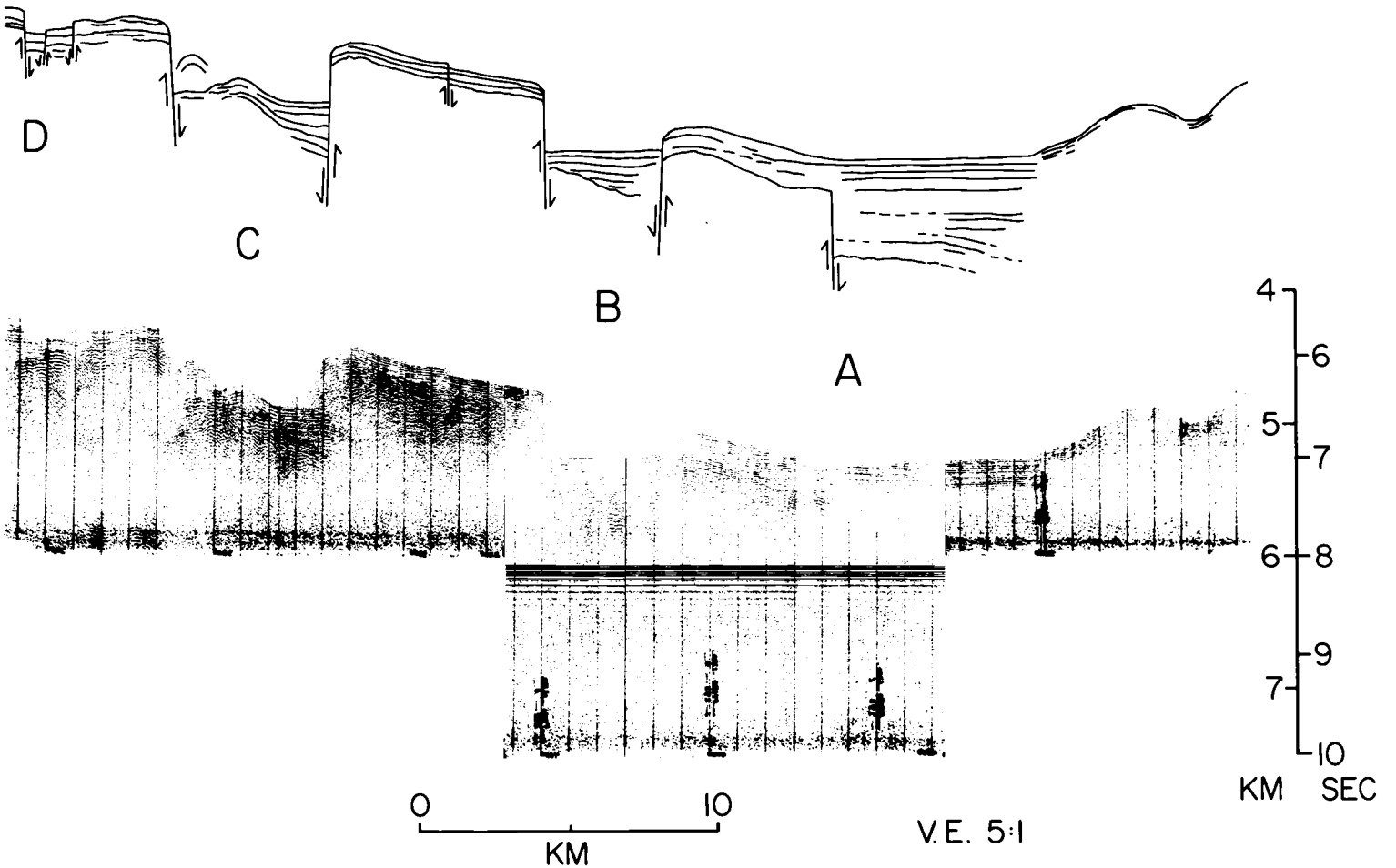

Figure 16. Seismic reflection profile at 34°S showing normal faulting beneath thick axial turbidites (A, B) and on the seaward trench slope (C, D).

The depth of acoustic basement in the trench axis shallows just north of 33 °S. This is probably the main cause of the large step in axial depth (Figure 6), and also controls the level of ponded sediments in the trench axis south of 33 °S. Gradual landward bulging of the seaward trench slope, rather than vertical faulting within the axis, seems to be responsible for the shallowing of basement. This bulge may be related to the eastward extension of the line of seamounts containing the Juan Fernandez Islands (Figure 1).

Submarine canyons appear for the first time on the continental slope at 33 °S and are common south of this latitude. A major canyon heads just seaward of several small river mouths south of Valparaiso, meanders across the continental shelf and upper slope, then makes two right-angle turns before joining the axis (Figures 14 and 15). The canyon has a relief of up to 1000 meters, becoming greatest on the steep lower continental slope. The abruptness of the changes in the canyon's trend strongly suggests structural control, particularly within the 2000 to 3000 meter continental slope depths.

The simultaneous appearance of canyons and thick axial sediments correlates well with an increasingly humid climate on land. Relationships between axial trench fill, land climate, and continental shelf sedimentation rates have been discussed briefly by Galli-Oliver (1969). The amount of rainfall along the Chilean coast increases gradually from arid conditions in the north to humid temperate in

central Chile. The amount of axial sediment in the adjacent trench also increases southward, but much more irregularly (Figure 17). It appears that much of the cause of this uneven distribution lies in structural barriers which inhibit the northward transport of sediment along the trench axis.

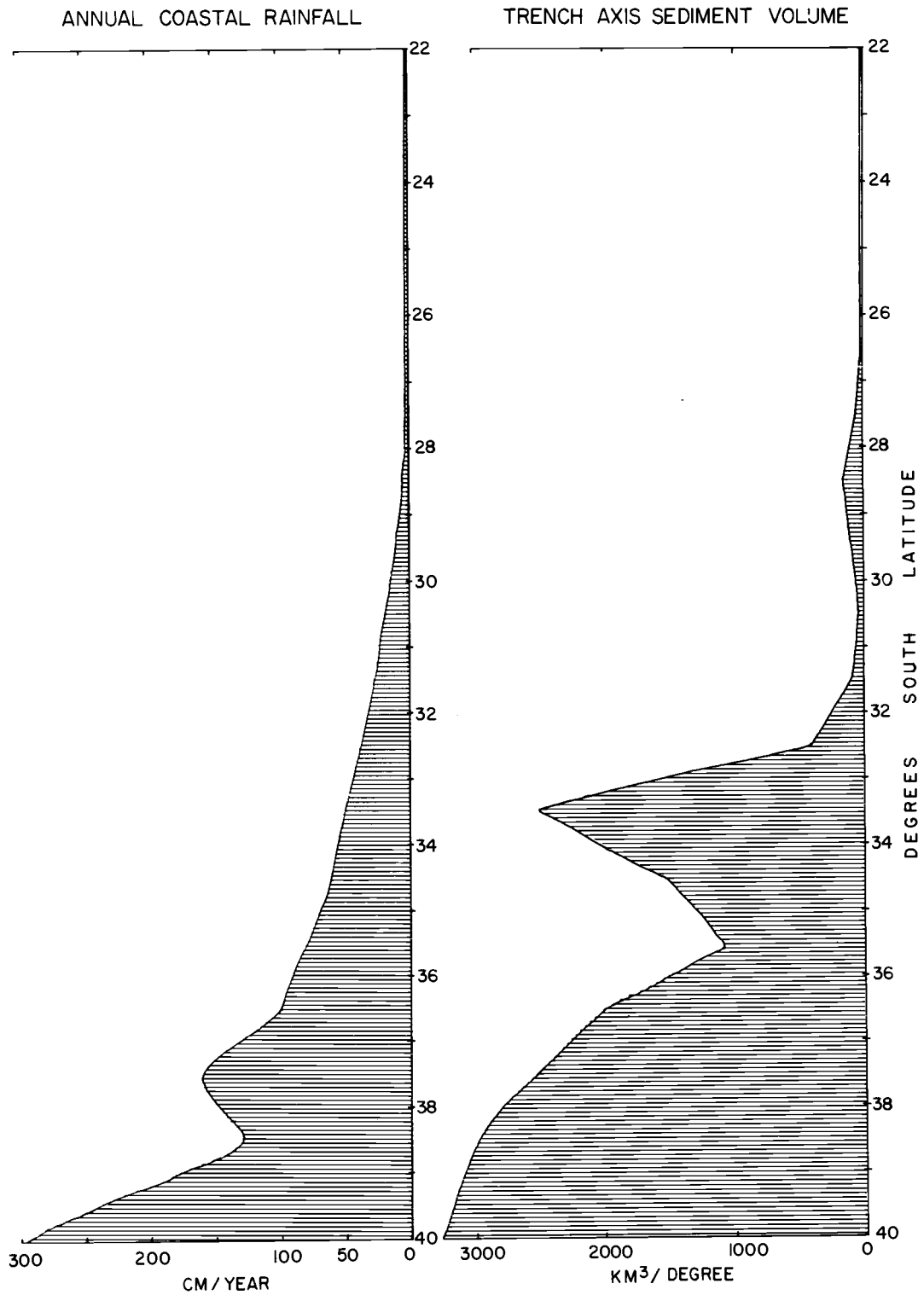

Figure 17. Comparison of trench sediment volume vs. rainfall on the adjacent coast of South America. The graphs show abrupt changes in sediment volume between trench provinces without corresponding sharp inflections in the rainfall distribution.

SEDIMENT TRANSPORT AND CONSUMPTION

The amount of sediment in the trench axis exhibits a regular stepwise increase from isolated ponds north of 27°S to a narrow, continuous axial wedge in the Central province and finally to a nearly filled trench south of Valparaiso (33°S). Galli-Oliver (1969) pointed out the close correlation of sedimentary fill in the trench to the climate on the adjacent continent (Figure 17), implicity assuming minimal north-south sediment transport in the trench axis. Scholl et al. (1970) similarly asserted that "contribution from southerly regions by northward flowing axial turbidity currents is only of secondary importance" (p. 1354). The intent of this discussion is to establish that, contrary to the above presumptions, a large part of the distribution of sediment in the axis of the Chile Trench can be accounted for by a model which uses only a southern source of sediments, transport of these sediments northward by turbidity current flows within the trench axis, and disappearance of the resulting deposits as a consequence of plate convergence.

Central Province: Assumptions and Calculations

The best test region for the above hypothesis is the narrow axial sediment wedge of the Central Province. If a steady state (constant total volume through time) of sediment fill is being

maintained in this section of the axis, the rate of removal of sediment due to convergence must be equal to the volume of sediment supplied by turbidity flows. Axial morphology and sediment type distributions (see Geologic Samples and Southern Province sections) strongly indicate northward flow and probable significant sediment transport by turbidity currents through the structural constriction at 33°S. The actual volume of transport past this point is impossible to measure directly, since it occurs in intermittant pulses. However, it is reasonably simple to estimate the volume of sediment contained within the axial sediment wedge on the basis of bathymetry and seismic reflection data, and likewise to obtain a rate for removal of axial sediments from sediment thicknesses and published convergence rates. Finally, average volumes for single turbidites, based on core data, can be used to calculate the periodicity of flows necessary to balance removal by subduction.

One further assumption is that the constrictions in the trench axis, particularly at 33°S, are relatively permanent features in the present sediment distribution system. The topic of changing configurations of the trench is further discussed in the next section.

Although complex, obscure processes are involved in subduction, material carried against the base of the continental slope can be thought of as being either accreted onto the slope or subducted beneath it. In either case, the sediment disappears from the axial

wedge at a rate proportional to its thickness at the base of the slope. The landward edge of the axial wedge can be visualized as a front of deformation which advances over the oceanic plate with time (Helwig and Hall, 1975). Assuming a right triangular prism for the shape of the sediment wedge, the volume of trench axis sediment removed in a given time interval along a section of trench axis is equal to the base-of-slope axial sediment thickness multiplied by the length of the trench section multiplied by the horizontal plate convergence over the desired time interval (Figure 18).

Applying this formula to the Central Province, the average base-of-slope thickness between 32°30'S and 27°30'S, corresponding to a wedge length of 550 km, is 200 to 400 meters. Using Minster et al.'s (1974) convergence rate of 10 cm/yr, the rate of removal is 1.1 to $2.2 \times 10^7 m^3/yr$, or roughly 1 to 2 km^3 per 100 years (Table 1). This compares to a total axial wedge volume of 2.8 to $5.6 \times 10^{11} m^3$ for the same segment, indicating an average residence time of 1400 to 5600 years for sediments in the axis.

Piston cores from this area indicate that individual turbidite layers range from 5 to 25 cm thick. Assuming that the deposit from a single flow covers the 3000 km^2 surface of this axial basin with an average of 10 cm of sediment, the sediment load of a single deposit would be $3 \times 10^8 m^3$, or about one-third of a cubic kilometer. This volume is well below the values for sediment loads of individual

PARAMETERS

L = length of wedge
h = sediment thickness
C = horizontal convergence rate
T_0 = Initial position of the deformation front
T_1 = Position of deformation front after a given time interval
$\Delta w = (T_1 - T_0) \cdot C$
V_S = volume of sediments removed

Formula For Volume Of Sediment Removed

$V_S = L \cdot h \cdot \Delta w = L \cdot h \cdot (T_1 - T_0) \cdot C$

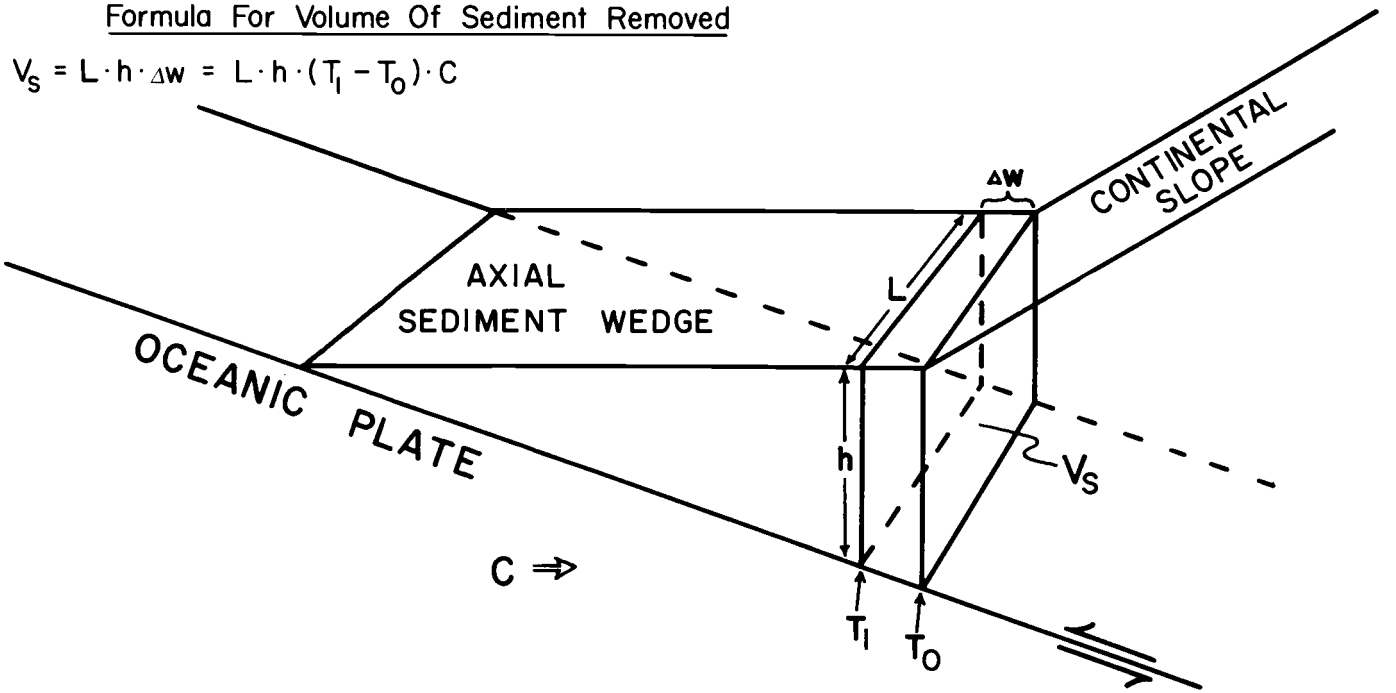

Figure 18. Diagram illustrating method of calculation of rate of consumption of axial sediments due to plate convergence. See Table 1 for calculations.

TABLE 1. Sediment Transport and Consumption Balance

Data	Value Used	Range
a) Surface area of axial sediment pond between 32°30'S and 27°30'S	3000 km^2	± 300 km^2
b) Thickness of axial sediment wedge	200 - 400 m	100 - 500 m
c) Width of axial sediment wedge	5 km	2 - 6 km
d) Convergence rate (Minster et al., 1975)	10 cm/yr	± 1 cm/yr

Calculations

A) Volume of axial sediments (see Figure 18)

low estimate: $V = \frac{1}{2} \times (5° \times 111 \text{ km}/°) \times 5 \text{ km} \times 200 \text{ m}$
$= 2.8 \times 10^{11} m^3$

high estimate: $V = \frac{1}{2} \times (5° \times 111 \text{ km}/°) \times 5 \text{ km} \times 400 \text{ m}$
$= 5.6 \times 10^{11} m^3$

B) Consumption due to convergence (see Figure 18)
(= convergence rate times thickness of sediment times wedge length)

low estimate: $C = 10 \text{ cm/yr} \times 200 \text{ m} \times 555 \text{ km}$
$= 1.1 \times 10^7 m^3/yr$

high estimate: $C = 10 \text{ cm/yr} \times 400 \text{ m} \times 555 \text{ km}$
$= 2.2 \times 10^7 m^3/yr$

C) Volume of a single turbidity flow deposit

= average thickness of a single flow times area of sediment basin

$= 10 \text{ cm} \times 3000 \text{ km}^2 = 3 \times 10^8 m^3$

TABLE 1, Continued

D) Necessary frequency of turbidity flows to balance consumption (= volume of one turbidite divided by the consumption rate)

low estimate: $F = 3 \times 10^{8} m^{3} / 1.1 \times 10^{7} m^{3} yr^{-1} = 27$ years

high estimate: $F = 3 \times 10^{8} m^{3} / 2.2 \times 10^{7} m^{3} yr^{-1} = 14$ years

turbidity flows estimated by Bennetts and Pilkey (in press) for a study of turbidite deposition off the Bahama Islands. Although dissimilarities in many factors (sediment type, tectonic setting, etc.) make comparison of turbidity current deposition in the two regions difficult, the southern Chile continental shelf is a larger area subject to more fluvial input than the Bahama Platform. Single flows supplied to the Chile Trench might therefore be expected to be at least as large as those measured in the Bahamas. The volume of sediment needed for a single flow in the Central Province could be supplied by a portion of a large flow originating in the Southern Province. The deep-sea channel in the axial sediments south of 33°S (Figure 13) is evidence that some excess material flows north past 33°S. From the above calculations, one "typical" flow is required every 14 to 27 years to balance the amount of sediment removed from the Central Province axial wedge by tectonic processes related to convergence.

Continentally-derived sediments supplied to the continental shelf and slope south of Valparaiso (33°S) provide an ample source for these turbidites. Submarine canyons heading near river mouths and leading across this broad shelf provide paths of transport down the continental slope to the trench axis (Kulm, unpublished research). Even assuming shelf sedimentation rates much lower than the one meter per century documented by Galli-Oliver (1969), the volume of sediment available from the shelf and upper slope to the trench is

orders of magnitude more than needed for maintaining a steady state of fill in the Central Province.

Kelleher (1972) found the periodicity of major earthquakes along this seismically active margin to be on the order of one every fifty years while minor tremors are much more frequent. These shocks furnish excellent mechanisms for remobilizing the rapidly accumulating shelf and upper slope deposits in the south, triggering slumping and formation of turbidity flows. Uplift of the outer continental shelf (Lomnitz, 1969) may also contribute to potential removal of sediment by steepening of the upper slope.

The volume of material passing down the trench axis should diminish progressively north of the present 33°S constriction because of continual deposition from each flow as it proceeds northward down the trench axis. Thus, while a sediment flux of 1 to 2 km^3 per century is required at 33°S, only about one-half that amount would probably pass 30°S, and far less would be needed at the northern end of the Central Province. Blockage of flows by the present obstruction at 27°30'S abruptly terminates the continuous axial wedge, impeding down-axis deposition that would otherwise occur north of this latitude.

Whole-Trench Sedimentation Model

Using these data, a simple model can be formulated to explain many characteristics of the distribution of sediments in the Chile

Trench axis. The general features of this model can be followed on the series of bathymetric profiles (Figure 11). South of Valparaiso (33°S), high rates of sedimentation on the continental shelf and slope provide an ample source for turbidites which nearly fill the trench (profiles 14 and 15). Excess material is channeled northward along the outer part of the turbidite pond until it flows through the constriction separating the Southern and Central Provinces (profile 13). Here the flows temporarily become erosional due to the steepened axial gradient, then revert back to a depositional mode as they spread over the level trench floor between 32°30'S and 27°30'S (profiles 6-12). North of 27°S, the supply of sediment from axial flows is not enough to maintain an appreciable axial sediment wedge against the combined effects of convergence and structural blockages. The result is a series of small basins separated by sections of trench axis barren of ponded turbidites (profiles 1-5).

The response of this system to an increase in sediment supply due to larger or more frequent turbidity flows, for instance during a glacial maximum, would be a general northward shifting of the boundary between the Central and Northern Provinces, with a concurrent slight thickening of the Central Province sediment wedge. Present structural control of the transition zone at 33°S would inhibit a similar northward shift of the Central-Southern boundary, but the rate of sediment transport through this constriction would increase.

Reversion of sedimentation rates to the lower interglacial values would be followed by shrinking of the axial sediment wedge because the consumptive effects of plate convergence would exceed the diminished rate of sediment supply by turbidity flows.

Long Term Effects

Assuming that the present thickness of axial sediments is representative of the average thickness over geologic time, it is possible to calculate the volume of trench axis sediment consumed or removed over long periods. At the steady-state rate of removal of 1.1 to 2.2 x 10^7 m^3/yr along the Central Province, 11,000 to 22,000 km^3 of sediment per million years (m.y.) is supplied to the trench axis.

On the basis of the conservative 11,000 km^3/m.y. estimate, a serious long-term deficiency in accreted continental slope material exists in the Central Province. The entire volume of the continental margin from the shoreline to the trench axis above the projected surface of a descending oceanic plate dipping 10° can be accounted for by 25 million years of only accretion of all sediments supplied to the axis (assuming no compaction and no contribution by hemipelagic sedimentation on the slope). Since subduction in the Peru-Chile Trench apparently has been active over the past 125 million years (McNutt et al., 1975), a potential volume of sediments several times greater than the total possible accreted section present in the

continental slope should have been supplied to the trench axis in this region. In addition, crystalline Paleozoic rocks along the coast strongly suggest that part, and perhaps most of the continental slope is composed of older rocks associated with the continental block, and not of accreted sediments. This would increase the problem of a lack of accreted section.

Two obvious solutions exist for resolving this mass imbalance: either the average supply of sediment to the trench axis in the past was nearly an order of magnitude lower than at present, or most of the sediments removed from the trench axis have been subducted to a position deep beneath the continental block along with the oceanic lithosphere. Although the present trench axis fill may represent relatively high sedimentation rates from the last glacial maximum, the order of magnitude sedimentation rate change needed to reconcile the imbalance would be a drastic alteration. On the other hand, McNutt et al. (1975) suggests that subduction of substantial quantities of oceanic sediments would help to explain a systematic increase of $^{87}Sr/^{86}Sr$ ratios with decreasing age of Andean volcanic and plutonic rocks in northern Chile. Although there is no unequivocal evidence to support or disprove either hypothesis, subduction of sediments is the more tenable of the two.

Finally, it must be kept in mind that any structural features riding on the oceanic plate or developed within the trench have a

relatively brief residence time in the trench before being subducted. At 10 cm/yr convergence, the transit time of a single point on the oceanic plate to go from the outer slope break to the landward edge of the trench axis only amounts to about 500,000 years. Considering only the 5 km average width of the trench axis, this term reduces to a mere 50,000 years. Consequently, province boundaries which are in part controlled by tectonic blockages associated with the downgoing oceanic crust are transitory features in the evolution of the continental margin.

STRUCTURAL PATTERNS

Any major deformation of the earth's crust should be explainable as a mechanical response to stresses acting on rock materials in a predictable manner. Although a large volume of published descriptions of trench morphology and shallow structure exists, almost no attention has been given to the stresses necessary to form the various structures. The following section combines well-known structural principles with published data on seismicity and stresses and the structural data presented in this paper to produce a model explaining deformation of the descending oceanic plate within the Chile Trench.

Stress notations in this section follow the common usage of a three-dimensional orthogonal set of stress vectors in which $\sigma_1 > \sigma_2 > \sigma_3$. The intermediate stress vector, σ_2 , is assumed to be horizontal and uniform paralleling the trench axis, and is not discussed in the analysis of cross-trench stress systems.

Extensional Rupture of the Oceanic Crust

Horst and graben features occur at several sites along the Chile Trench (Figures 8, 9, and 10). They can also be recognized in bathymetric and seismic reflection profiles from several other deep-sea trenches (Raitt et al., 1955; Fisher and Hess, 1963; Ross and Shor, 1965; Ludwig et al., 1966). In most of these studies,

normal or step faulting of blocks of oceanic crust downthrown toward the trench axis is described as the dominant means of deformation (Figure 19A). The single exception is the work of Ludwig et al. (1966) in which graben faults are attributed to tensional forces from bending of a static oceanic crust due to sediment loading of its landward edge. Prince (1974) and Prince and Kulm (1975) revised the earlier step-fault models with a version that explains compressional faulting and uplift of sections of ocean crust in the trench axis within the framework of plate tectonics (Figure 19B). The model proposed here (Figure 19C) is similar in some respects to both of the above, but assumes a dynamic ocean crust and uses theoretical studies of stress and failure to predict patterns of faulting.

A simple semi-elastic slab, when bent along a hinge line, will develop an upper zone of extension and a lower zone of compression separated by a neutral plane of zero net horizontal stress (Johnson, 1970, p. 53). For a uniform, weightless bending slab under no horizontal regional stress field, the neutral plane will lie near the middle of the slab (Figure 20A). Addition of a regional field of horizontal compressive stress normal to the hinge line will shift the netural plane to a shallower depth within the slab, but a zone of tension will persist above this plane (Figure 20B).

In the oceanic plate, the lithostatic stress field (stresses due to the weight of overlying rock and water) must be added to the stresses

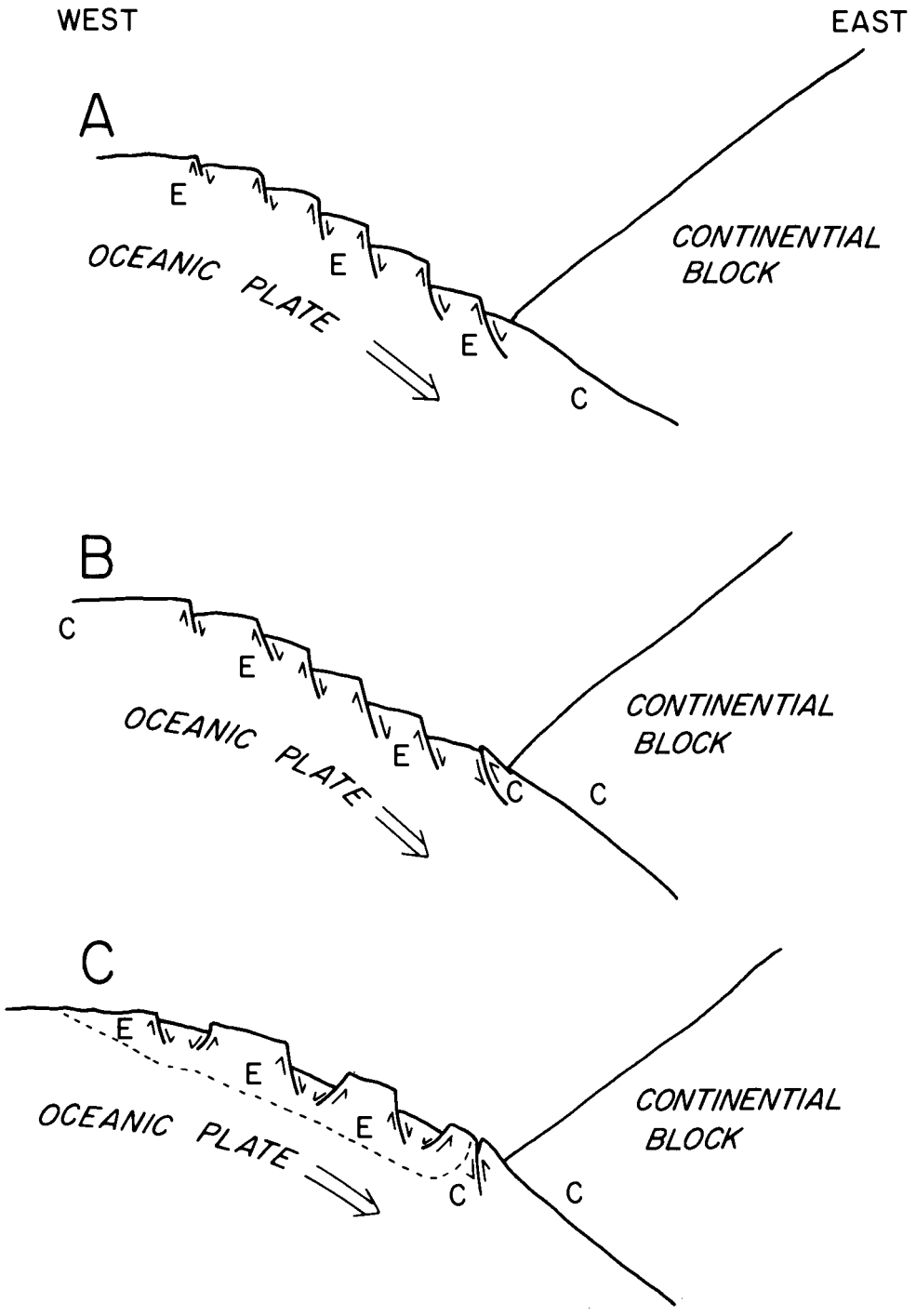

Figure 19. Various models for rupture of the oceanic plate prior to subduction. See text for discussion.

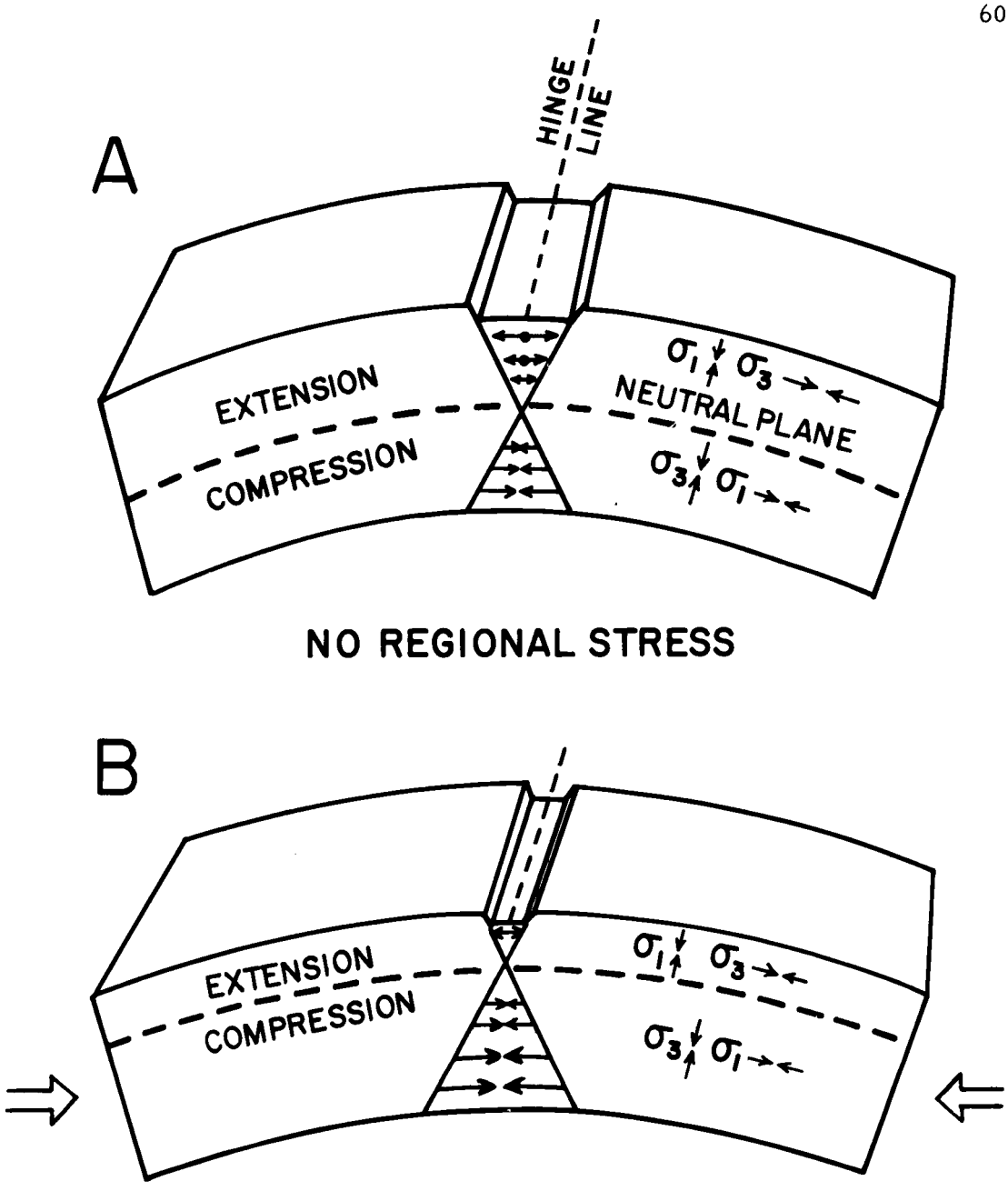

Figure 20. Schematic diagram of a bending semi-elastic slab (A) under no horizontal stress field, and (B) with a stress field compressive normal to the hinge line. Surface displacements on the blocks are typical responses to tension. (After Johnson, 1970, Figure 8.5).

due to bending. Under these conditions, the neutral surface separates a lower region of compression (horizontal stress > vertical stress) from an upper region of extension (vertical stress > horizontal stress) rather than from a region of true tension ($\sigma_3 < 0$).

The preferred fault patterns for a stress system similar to that created in a bending slab were analyzed by Hafner (1951), taking into account the effect of lithostatic stress increasing with depth. The vertical distribution of stresses in the central portion of Figure 21 is essentially identical to that produced by bending of an intially planar slab. Normal faulting with steep dip angles is predicted at the surface, although the dip angle may curve and either flatten or steepen at depth. Faults which dip toward each other at the surface tend to intersect at a depth proportional to their horizontal separation at the surface.

The oceanic lithosphere can be modeled as an elastic slab about 75 km thick with considerable rigidity and a consequent ability to maintain and transmit stresses (Walcott, 1970). The scant information on shallow-focus earthquakes on the Nazca Plate (Mendiguren, 1971) and the plate crustal structure (Hussong et al., 1975) indicate predominantly compressive stress in the oceanic crust seaward of the outer slope break. As the oceanic plate bends to descend beneath the continent, a zone of extension is produced in the upper portions of the oceanic crust. Faulting commences near the outer slope break

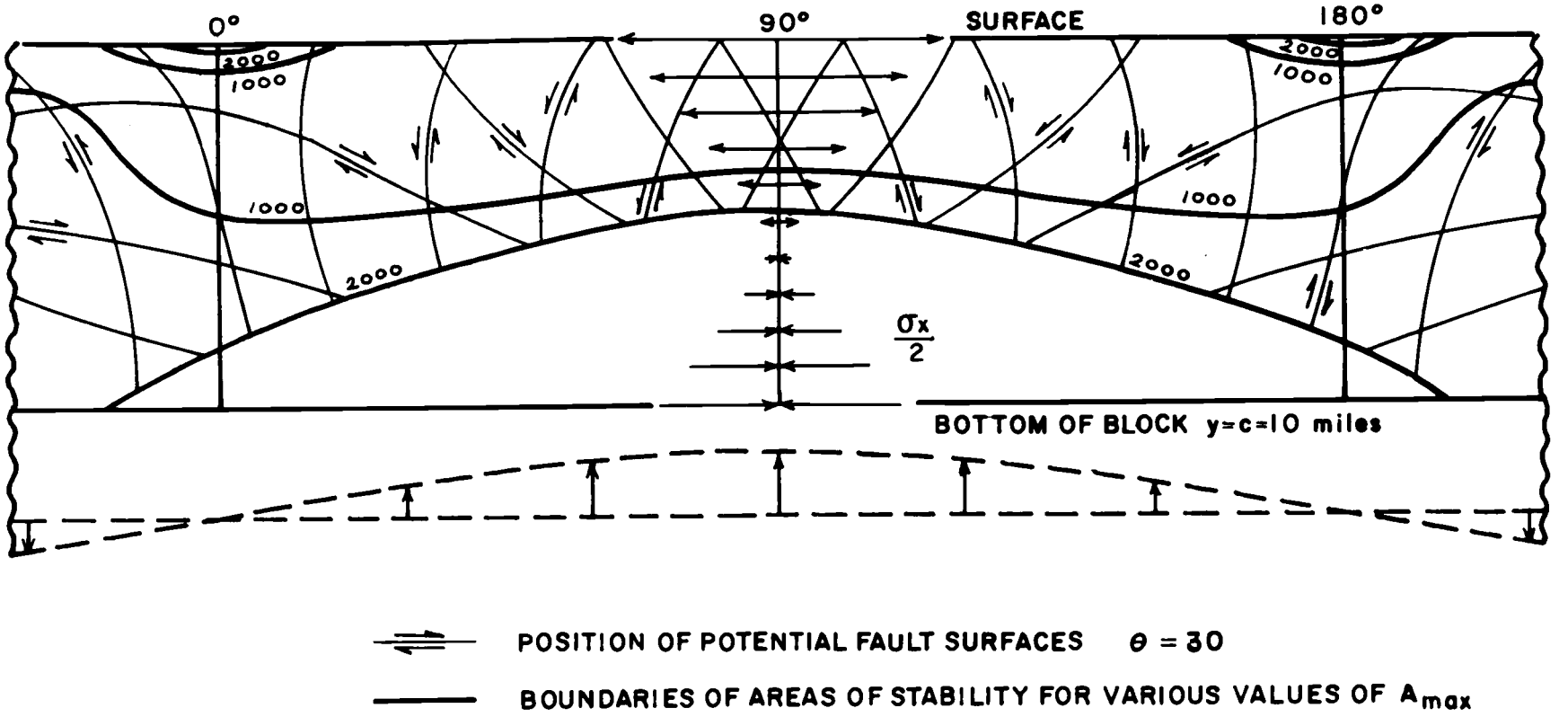

Figure 21. Preferred patterns of faulting due to a stress distribution similar to that created in a bending elastic slab (after Hafner, 1951).

(Figure 2) and increases in magnitude as the plate is bent more sharply downwards. Following the patterns predicted by Hafner (Figure 21), the faults dip approximately 60° at the surface but probably curve somewhat with depth. The resulting configuration of faults and the distribution of stresses is shown in Figure 19C.

Regional horizontal compression of the oceanic plate should cause the base of the zone of extension, due to bending, to be shallower than it would be in a plate under neutral horzontal stress. An estimate of the minimum depth of the zone of extension can be calculated using data from structural features assumed to be due to extensional faulting. Grabens on the seaward trench slope of the Northern Province (Figures 8 and 9) have floors 4 to 8 km wide bounded by steep fault scarps which should dip at typical normal-fault angles of 60° (Hubbert, 1951). These inward-dipping faults should intersect at a point beneath the graben floor within the zone of extension. Assuming non-curving faults, this depth for the above features should be 3.5 to 7 km below the graben floor. Curving of the faults in the manner predicted by Hafner (Figure 15) could alter this depth slightly either upwards or downwards. In any case, the zone of extension seems to extend down into oceanic layer three.

Horsts and grabens occur both in sections of trench lacking ponded sediments (Figure 9) and in regions nearly filled with turbidites over a kilometer thick (Figure 16), indicating that these

features occur independently of the presence or absence of axial sediments. No warping or faulting of the turbidites surrounding the faulted blocks in the filled sections of trench axis can be seen (Figures 10 and 16). This evidence argues for development of most of the fault offsets on the seaward slope before the plate encounters the axis. Both of these observations are in agreement with faulting caused by extension along the surface of a bending lithospheric plate.

Uplift of Oceanic Crust Near the Trench Axis

As the descending oceanic plate comes in contact with the continental slope, opposing plate motions apparently cause an abrupt reversal of stress within the oceanic crust from extensional seaward of the axis to compressional beneath the continental margin a few tens of kilometers landward of the trench axis. Solutions for shallow Chilean earthquakes are consistent with compressional failure below the upper continental slope and the Chilean coast (Stauder, 1973). However, the exact location of this stress reversal need not coincide precisely with the trench axis. The oceanic lithosphere has sufficient rigidity and strength to transmit sizable stresses over considerable distances (Walcott, 1970). Thus although the source of the compressive stress is well beneath the continental slope, it is not unreasonable to expect compression within the upper oceanic crust several kilometers seaward of the trench axis resulting from plate

collision.

Faulting in a uniform medium will occur first at the point of maximum differential stress ($\sigma_1 - \sigma_3$). If the horizontal stress along a plate is constant, compressional failure will occur first at the point of minimum vertical stress. In the absence of major faulting, the horizontal compressive stress in the upper oceanic crust due to plate collision should decrease gradually away from the effective point of contact below the continental slope. The lithostatic load on the surface of the oceanic plate undergoes a sharp increase at the trench axis, due to an increasingly thick wedge of relatively dense continental slope material overlying the plate. Under these conditions, the area of maximum differential stress will tend to roughly coincide with the trench axis despite the fact that the horizontal compressive stress is greater beneath the continental slope. Hence compressional failure of the oceanic crust in or near the trench axis is an entirely feasible mechanism for uplifting sections of trench sediments.

Lateral compression typically results in reverse faults with angles near 30° (Hubbert, 1951). However, the normal faults already present in the oceanic crust as it approaches the trench axis should dip 60° or more. These pre-existing normal faults constitute zones of weakness in the crust. If the frictional resistance to reversed motion is not excessive, some reversal of motion would be expected along these fault surfaces in response to the compressional stresses

from plate collision. Otherwise, newly-formed low angle thrusts would be expected in the upper sections of the basaltic crust. In either case, considerable disruption of the magnetized basalt in the upper crust along these compressional faults would result in attenuation of remnant magnetism seaward of the axis. This trend has been documented in a companion study of the Chile Trench by Hassanzadeh (1976).

Reverse or thrust faulting seaward of the base of the continental slope can result in sections of crust being uplifted in or near the trench axis. Prince and Kulm (1975) have documented uplift of 700 meters in 3100 years for turbidites on a basalt ridge in the axis of the Peru Trench, while the turbidites in the Central Province of the Chile Trench have undergone uplift of 350 meters in 5380 years.

The rates of uplift and convergence can be used to indirectly measure the angle of faulting, since the ratio of vertical to horizontal motions gives the tangent of the average dip angle of the fault. If the 22 cm/yr uplift rate in the Peru Trench is due solely to reverse faulting caused by plate convergence of 10 cm/yr (Minster et al., 1974), the angle of the main fault must be at least 65°. Similarly, the 6.5 cm/yr rate of uplift in the Chile Trench indicates a minimum fault angle of 33°. In the former case, reversed motion along an existing normal fault is a more plausible explanation for the uplift than a newly formed thrust fault dipping at an anomalously high angle.

The Chile Trench case can be accomplished either by continual low-angle (33°) thrusting during the entire 5380 years or episodic motion along a steeper fault over part of this time span.

Segmentation

In addition to structural features formed in response to stresses acting perpendicular to the trench, there are also major north-south changes in structure along the trench and continental margin which can be used to segment the trench into the provinces described previously (see Provinces and Features of the Trench). Various authors have proposed segmentation of the subducting Nazca Plate and the overriding South American continent on the bases of seismicity (Kelleher, 1972; Stauder, 1973; Swift and Carr, 1975), morphology (Hayes, 1966), land geology (Ruiz et al., 1965), or combinations of the above (Sillitoe, 1974). No overall scheme for segmentation has thus far emerged to fully explain these laditudinal variations in structure, seismicity and geology, nor do the positions of segment boundaries correlate well among studies which use different criteria for determining these boundaries.

The trench segments defined by this study on the basis of bathymetry and structure have boundaries at 27°S and 33°S (e.g. Figure 6). Stauder (1973) shows breaks in the seismic (Benioff) zone which can be extrapolated upward to the same latitudes in the trench.

There are also terminations in the Central Valley and in the Andean chain of recently active volcanoes at corresponding latitudes on the continent (Figure 1). However, mere geographical coincidence of these boundaries furnishes little useful information on the significance of trench segmentation. Better insights might be gained by examining possible causes of north-south changes in the combined trench-continental margin system.

One currently popular theory dealing with tectonics of subduction zones has developed from the observation that almost all trenches are arc-shaped in map view, convex toward the underthrusting plate. Frank (1968) noted that the oceanic plate is in a state of minimum stress when its angle of downward flexure is twice the radius of curvature of the arc on the earth's surface. Le Pichon et al. (1973) and Strobach (1974) expanded on this theme, predicting the stress patterns and resultant deformations of the downbending plate when the curvature of the trench does not conform to the minimum stress configuration.

The Chile Trench is conspicuously linear from 22°S to 27°S and is generally straight over its entire extent from 20°S to 40°S. As a consequence of this linearity, stresses within the descending slab are compressional parallel to the line of flexure of the plate; i.e. along the strike of the trench axis. Strobach (1974) predicted that the response to this stress should be curtain-like folding of the

descending slab.

One way to test the significance of this lateral stress and its implications on segmentation is to calculate the maximum possible strain within the oceanic slab due to subduction along a straight trench. Using equation (2) from Strobach (1974), compressive strains in the descending slab have been calculated for an oceanic plate dipping 20° (average value for the Chile seismic zone from Stauder, 1973) from a linear trench axis (Table 2). The maximum calculated strain on the oceanic plate only amounts to 1.5% (ε) at a depth (D) of 100 km. This depth on a plate dipping 20° lies about 250 km landward of the trench axis. It is unlikely that a strain of this small amount would be capable of significantly deforming the subducting lithosphere at this depth, and even less likely as the strain decreases to negligible values toward the trench axis. Distortion of the oceanic plate as a consequence of subduction along a linear trench may be important in producing segmentation of the descending plate at depth, but apparently has little or no effect on segmentation in or near the trench.

Two other possible controlling factors for segmentation of the trench are significant: (1) structure of the continental block, and (2) pre-existing lines of weakness in the oceanic plate, particularly fracture zones. The coincidence of the two major trench transition zones (27°S and 33°S) with terminations of major physiographic

TABLE 2. Calculation of Strain Due to a Linear Trench

Equation (2) from Strobach (1974):

$$\varepsilon = \frac{r_2 - r_1}{r_1} \approx \frac{1[\cos\beta - \cos(\alpha - \beta)]}{R_o \cdot \sin\beta - 1 \cdot \cos\beta} = \frac{1}{R_o} \cdot \frac{\cos\beta - \cos(\alpha - \beta)}{\sin\beta - \frac{1}{R_o}\cos\beta} \quad (2)$$

Figure 3 from Strobach

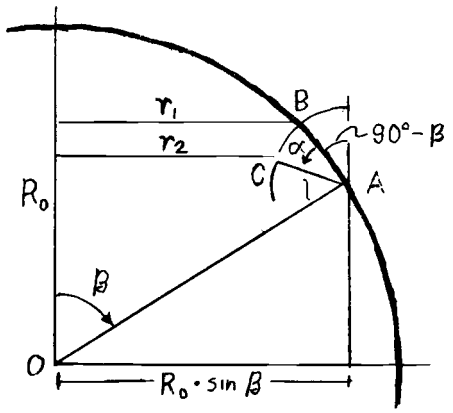

L = length of slab (in km)

β = radius of arc = 90° (linear trench)

α = dip angle = 20°

R_o = radius of earth

D = depth below earth's surface (vertical)

Results

L (km)	D (km)	ε (compressive strain) %
100	36	0.53
200	73	1.07
300	109	1.60
400	146	2.14
500	182	2.67

lineations on the continent (volcanoes and Central Valley) lends support to the former hypothesis. Insufficient data exist for the eastern Nazca Plate to adequately test the latter factor at present.

One prime consideration is that because of the rapid convergence rate, any feature associated with the oceanic plate has only an ephemeral influence on the juxtaposed continental margin. Thus, if intracontinental structures control trench segmentation, the transitions will remain fixed with respect to the margin. If, on the other hand, oceanic plate features control segmentation, the segment boundaries will change position fairly rapidly relative to geologic processes such as vulcanism and continental accretion.

PROPOSED MODEL

> There is something fascinating about science. One gets such wholesale returns of conjecture from such a trifling investment of fact.
>
> --Mark Twain

Possible Effects of Sediment Supply on Continental Accretion and Tectonic Erosion

Based on the above data and the resulting specific models for sedimentation patterns and structural styles within the trench, a rather speculative overall model for tectonics in the Chile Trench can be formulated. This model is predicted on the concept that the supply of sediment to the trench axis plays a major role in the tectonics of convergent margins.

A thick layer of sediment riding on an oceanic plate may be subjected to two processes as it collides with a continental block. The upper portion tends to be scraped off and added to the continental slope as a wedge of accreting sediment, while the bulk of the lower layers are thought to be carried down beneath the continent along with the descending oceanic plate. The importance of thick sequences of trench sediment to continental accretion has been shown by Seely et al. (1974) and Kulm and Fowler (1974). However, the role of subducted sediment in the structural evolution of a convergent margin has not been thoroughly explored. The question of what happens when

there is little or no sediment to subduct is particularly applicable to the Chile Trench.

Subduction of pelagic and hemipelagic sediments from the trench axis may form a water-saturated, clay-rich layer along the slippage plane between the rock masses of the colliding plates. The lubricating effect of this layer should reduce friction and smooth over some of the basement relief of the oceanic plate, allowing it to slip beneath the continental block with minimal resistance. Consequently, there is little breakup of the underside of the continental slope. Sediments that are not consumed by subduction are added to the continent, forming an accreted section which gradually builds outward from the original edge of the continent. The axis gradually migrates to a position further from shore, and becomes shallower since it is situated relatively higher on the seaward trench slope (Figure 22A).

In a few cases, such as the oceanic plate off northern Chile, the blanket of oceanic and trench sediments is not sufficient to cover the major basement relief of the oceanic plate even disregarding the large fault offsets commonly formed on the seaward trench slope. Without this buffer zone, irregularities up to several hundreds of meters would scrape directly against the underside of the continental slope as they are subducted. Considerable rupture of the rock units on both sides of the contact zone will gradually cause material from the underside of the continental slope to be broken up and removed

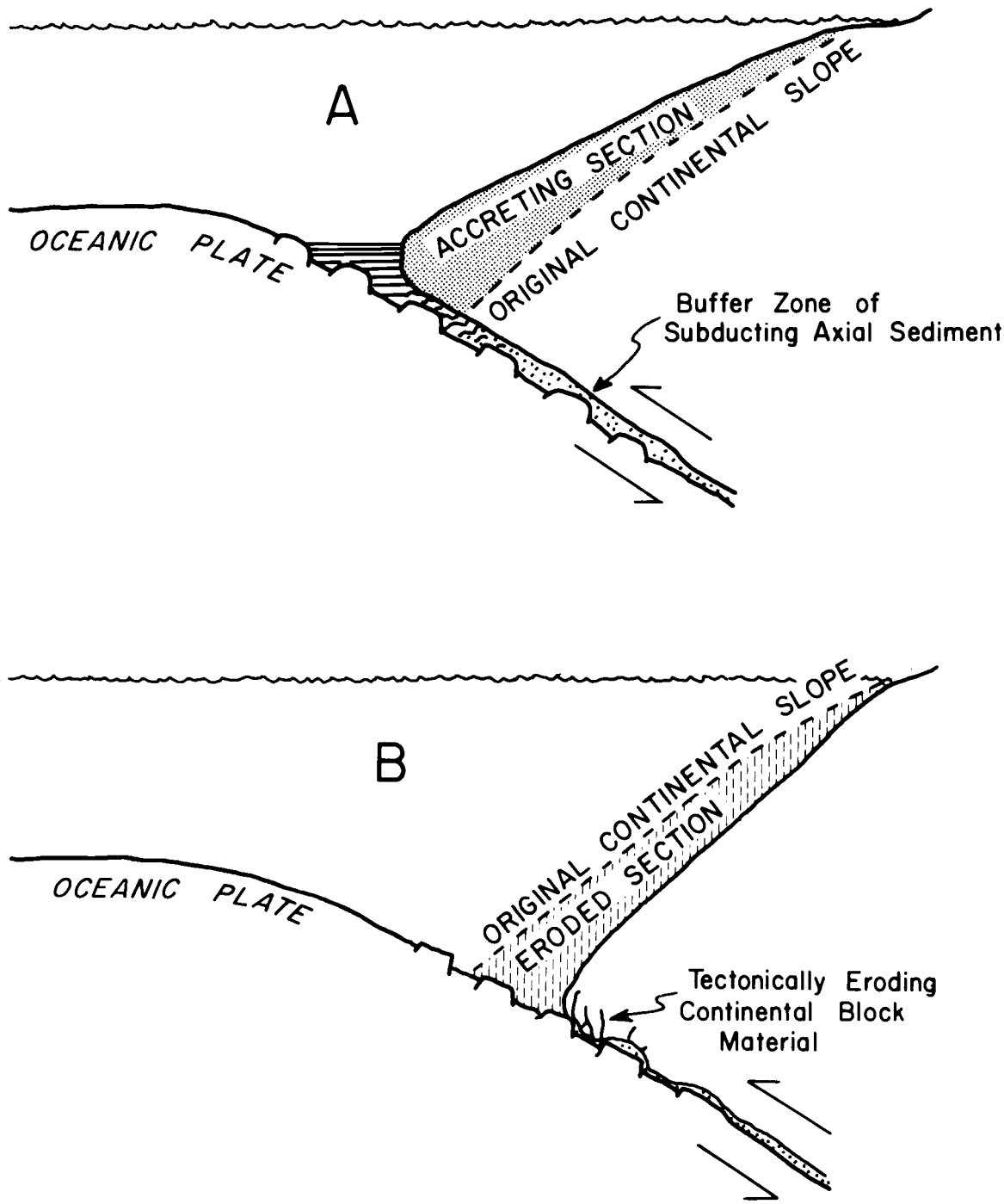

Figure 22. Diagram showing the prolonged effects of continental accretion (A) vs. tectonic erosion (B) on the evolution of the continental margin. The tectonic style is dependent on the amount of sediments available to the axis.

downward with the subducting plate.

Although actual rates of tectonic erosion will probably be very slow, removal of a few kilometers of continental slope over several tens of millions of years of active underthrusting does not seem unreasonable. Since this erosion would be most severe near the trench axis, the long-term effect would be to shorten and steepen the continental slope, particularly the lower portion. A slight deepening of the trench axis would occur as a consequence of exposure of more of the downbending oceanic plate (Figure 22B).

The data in this study strongly suggests that a correlation exists among sediment supply, trench depth, and continental slope morphology along the Chile Trench. The trench-slope break characteristic of the landward slopes of most western Pacific trenches (Karig, 1974) is present as a prominent mid-slope bench in the Central and Southern Provinces, but is absent in the Northern Province. Karig and Sharman (1975) proposed that this slope break is a morphologic feature created by an accreting prism of sediments in the lower slope. The indication is that accretion has occurred in the southern sections of the Chile Trench but not in the north.

The present distribution of axial sediments and the regional northward increase in trench depth both support this hypothesis. Where thick sequences of sediments fill the trench axis, the continental slope is broad and the basement depth of the trench axis

(sediments removed) is relatively shallow. Proceeding northward, the amount of sediment in the axis dwindles to nearly zero north of 27°S. Simultaneously, the overall gradient of the continental slope steepens, benches diminish, and the basement trench depth reaches a maximum. Since there is no appreciable change in tectonic setting (convergence rate or angle) along this margin, the dominating factor seems to be the changing amount of sediment supply.

Tectonic removal of up to 200 km of continental material from the western edge of South America along northern Chile during the past 200 million years has been suggested by various authors from several lines of geologic and geochemical evidence (Miller, 1970; Arabasz, 1970; Rutland, 1971). Although tectonic erosion seems to be a feasible process in the northern province of the Chile Trench, the amount of continental margin destroyed in this manner is probably minimal. The long-term effect is more a control of the morphology of the continental slope rather than a major reshaping of the outline of the continent.

SUMMARY AND CONCLUSIONS

Most of the major features of the Chile Trench can be explained by the interactions of a few fairly simple, readily definable processes. The three main agents at work are the supply of continental sediments to the trench axis via turbidity flows, the bending of the oceanic plate prior to subduction, and the underthrusting of the oceanic crust beneath the South American continental block.

The Nazca Plate moves approximately due east toward South America at 10 cm/yr (Minster et al., 1974). As it approaches the continent, the oceanic plate begins to bend downwards to descend beneath the thick continental lithosphere under the Andes. A zone of extension is produced in the upper layers of oceanic crust as a consequence of this bending, overcoming the compressional stresses present in the relatively undisturbed central regions of the Nazca Plate.

Normal faulting due to this extension is initiated near the line of flexure (the outer slope break) and soon develops into large block-fault features, interpreted as horsts and grabens. Offsets of 500 to 1000 meters along steeply dipping faults are characteristically developed on the portion of the seaward slope in the 4000 to 5000 meter depth range, and do not become noticably larger with increasing water depth. Faulting is most frequently seen in the deeper

bathymetric portions of the trench north of 27°S (Figure 8), but can be seen even in the sediment-filled axis south of 34°S (Figure 16). The general lack of deformation of the layered sediments surrounding these partially buried fault blocks in the trench axis supports the hypothesis that most of the development of the normal faults occurs fairly high on the seaward trench slope, and not within the trench axis.

The extensional crustal rupture of the oceanic plate can be explained by a model based on failure patterns predicted for a bending semi-elastic slab. Flexure of a thick plate should produce a zone of extension along the convex surface of the plate. Both theoretical and model studies predict that preferred failure planes will dip about 60°, which is compatible with the data from the Chile Trench. Based on horizontal dimensions of the fault blocks and expected angles of faults, the zone of extension probably extends through the upper few kilometers of the Nazca Plate.

The present trench can be divided into three provinces (North, 23° to 27°S; Central, 27°S to 33°S; and South, 33°S to beyond 34°S) on the basis of combined structural and bathymetric trends of the trench axis and both trench slopes. Characteristics such as morphology of the continental slope, trench depth, axial sediment thickness, and degree of rupture of the oceanic plate remain relatively uniform within each province, but change abruptly at the

transition zones between provinces at 27°S and 33°S.

Sediment distribution along the trench axis is strongly influenced by the position of these province boundaries, which are related to tectonics of the colliding plates. High rates of sedimentation on the continental shelf and upper slope south of 33°S provide an ample supply for the turbidites which nearly fill the trench axis in the Southern Province. The level of this axial fill is maintained by a structurally constricted zone in the axis at 33°S, which restricts but does not totally block sediment transport longitudinally down the axis to the north. The diminished volume of sediment transport into the Central Province via axial turbidity current flows is still large enough to maintain a narrow, continuous wedge of horizontally layered sediments against the effects of plate convergence. Another partial structural blockage of the trench axis at 27°S terminates the present domain of turbidite deposition.

Between 23°S and 27°S, the trench axis consists of several small, isolated basins of horizontally layered sediment, separated by shallower areas containing no visible axial sediments. These ponds are thought to be remnants from an older era of higher sediment input to the trench axis.

At one locale (30°35'S), turbidites which were deposited in the trench axis are now found on the seaward trench slope elevated more than 350 meters above the present level of the axis. Regional

bathymetry and structure support local uplift of this site rather than regional downdropping of the axis. Radiocarbon dating of the uppermost turbidite sets the initiation of uplift at 5380 ± 350 years B. P., which gives a minimum rate of vertical movement of 6.5 cm/yr.

A correlation is seen between trench axis sediments and morphology of the adjacent continental slope. In sections of trench with thick axial sediment wedges (Southern Province), the continental slope is typically broad and interrupted by large benches. Where the axis contains little or no axial sediment (Northern Province), the slope is steeper and benches are not well developed. Thus the supply of sediment to the trench axis seems to play a major role in determining the tectonic style of the continental margin. An abundance of axial sediment apparently results in addition or accretion of material to the continental slope. Absence of sediment prevents formation of a buffer layer between the opposing plates, and may result in a non-accreting margin or ultimately lead to gradual tectonic erosion of the margin.

BIBLIOGRAPHY

Arabasz, W., Jr., 1971, Geological and geophysical studies of the Atacama fault zone in northern Chile (Ph. D. dissertation): California Institute of Technology, 275 numb. leaves.

Bandy, O. L., and Rodolfo, K. S., 1964, Distribution of foraminifera and sediments, Peru-Chile Trench area: Deep-Sea Research, v. 11, p. 817-837.

Bennetts, K. R. W., and Pilkey, O. H., 1976, Characteristics of three turbidites: Hispaniola-Caicos Basin: Geol. Soc. America Bull., in press.

Casertano, L., 1963, General characteristics of active Andean volcanoes and a summary of their activities during recent centuries: Bull. Seismol. Soc. America, v. 53, p. 1415-1433.

Coulbourn, W. T., and Moberly, R., 1976, Structural evolution of forearc basins off southern Peru and northern Chile: submitted to Canadian Jour. Earth Sci.

Farrar, E., Clark, A. H., Haynes, S. J., Quirt, G. S., Conn, H., and Zentilli, M., 1970, K-Ar evidence for the post-Paleozoic migration of granitic intrusion foci in the Andes of northern Chile: Earth and Planet. Sci. Letters, v. 10, p. 60-66.

Fisher, R. L., and Hess, H. H., 1963, Trenches, in The Sea, vol. 3, M. N. Hill, ed.: New York, Interscience, p. 411-436.

Fisher, R. L., and Raitt, R. W., 1962, Topography and structure of the Peru-Chile Trench: Deep-Sea Research, v. 9, p. 423-443.

Frank, F. C., 1968, Curvature of island arcs: Nature, v. 220, p. 363.

Galli-Oliver, C., 1969, Climate--a primary control of sedimentation in the Peru-Chile Trench: Geol. Soc. America Bull., v. 80, p. 1849-1852.

Grow, J. A., and Bowin, C. O., 1975, Evidence for high-density crust and mantle beneath the Chile Trench due to the descending lithosphere: Jour. Geophys. Research, v. 80, p. 1449-1458.

Hafner, W., 1951, Stress distributions and faulting: Geol. Soc. America Bull., v. 62, p. 373-398.

Hassanzadeh, S., 1976, Determination of depth to the magnetic basement using maximum entropy with application to the northern Chile Trench (M.S. thesis), Corvallis, Oregon State University, 64 numb. leaves.

Hayes, D. E., 1966, A geophysical investigation of the Peru-Chile Trench: Marine Geology, v. 4, p. 309-351.

Helwig, J., and Hall, G. A., 1974, Steady-state trenches?: Geology, v. 2, p. 309-316.

Herron, E. M., 1972, Sea-floor spreading and the Cenozoic history of the east-central Pacific: Geol. Soc. America Bull., v. 83, p. 1671-1692.

Hubbert, M. K., 1951, Mechanical basis for certain familiar geologic structures: Geol. Soc. America Bull., v. 62, p. 355-372.

Hussong, D. M., Odegard, M. E., and Wipperman, L. K., 1975, Compressional faulting of the oceanic crust prior to subduction in the Peru-Chile Trench: Geology, v. 3, p. 601-604.

James, D. E., 1971, Plate tectonic model for the evolution of the central Andes: Geol. Soc. America Bull., v. 82, p. 3325-3346.

Jenks, W. F., 1956, Handbook of South American geology: New York, Geol. Soc. America Mem. 65, p. 236-239.

Johnson, A. M., 1970, Physical processes in geology: San Francisco, Freeman, Cooper & Company, 577 p.

Karig, D. E., 1974, Evolution of arc systems in the western Pacific: Annual Review of Earth and Planetary Sciences, v. 2, p. 51-75.

Karig, D. E., and Sharman, G. F., 1975, Subduction and accretion in trenches: Geol. Soc. America Bull., v. 86, p. 377-389.

Kausel, E., and Lomnitz, C., 1968, Tectonics of Chile, in Pan-American symposium on the upper mantle, Mexico: Instituto Geofisica, U.N.A.M., p. 47-67.

Kelleher, J. A., 1972, Rupture zones of large South American earthquakes and some predictions: Jour. Geophys. Research, v. 77, p. 2087-2103.

Kulm, L. D., Scheidegger, K. F., Prince, R. A., Dymond, J., Moore, T. C., Jr., and Hussong, D. M., 1973, Tholeiitic basalt ridge in the Peru Trench: Geology, v. 1, p. 11-14.

Kulm, L. D., and Fowler, G. A., 1974, Oregon continental margin structure and stratigraphy: A test of the imbricate thrust model, in Burk, C. A., and Drake, C. L., eds., The Geology of Continental Margins: New York, Springer-Verlag, p. 261-283.

Kulm, L. D., Resig, J. M., Moore, T. C., Jr., and Rosato, V. J., 1974, Transfer of Nazca Ridge pelagic sediments to the Peru continental margin: Geol. Soc. America Bull., v. 85, p. 769-780.

Le Pichon, X., Francheteau, J., and Bonin, J., 1973, Developments in Geotectonics, 6, Plate Tectonics: Elsevier, New York.

Lister, C. R. B., 1971, Tectonic movement in the Chile Trench: Science, v. 173, p. 719-722.

Lomnitz, C., 1969, Sea-floor spreading as a factor of tectonic evolution in southern Chile: Nature, v. 222, p. 366-369.

Ludwig, W. J., Ewing, J. I., Ewing, M., Murauchi, S., Den, N., Asano, S., Hayakawa, M., Asanuma, T., Ichikawa, K., and Noguchi, I., 1966, Sediments and structure of the Japan Trench: Jour. Geophys. Research, v. 71, p. 2121-2137.

Mammerickx, J., Anderson, R. N., Menard, H. W., and Smith, S. M., 1975, Morphology and tectonic evolution of the east-central Pacific: Geol. Soc. America Bull., v. 86, p. 111-118.

Masias, J. A., 1975, Morphology, shallow structure, and evolution of the Peruvian continental margin, 6° to 18°S (M.S. thesis): Corvallis, Oregon State University, 92 numb. leaves.

McNutt, R. H., Crocket, J. H., Clark, A. H., Caelles, J. C., Farrar, E., Haynes, S. J., and Zentilli, M., 1975, Initial $^{87}Sr/^{86}Sr$ ratios of plutonic and volcanic rocks of the central Andes between latitudes 26° and 29° South: Earth and Planet. Sci. Letters, v. 27, p. 305-313.

Mendiguren, J. A., 1971, Focal mechanism of a shock in the middle of the Nazca Plate: Jour. Geophys. Research, v. 76, p. 3861-3879.

Miller, H., 1970, Das Problem des hypothetichen "Pazifischen Kontintes" gesehen von der chilenischen Pazifikküste: Geologische Rundschau, v. 59, p. 927-938.

Minster, J. B., Jordan, T. H., Molnar, P., and Haines, E., 1974, Numerical modeling of instantaneous plate tectonics: Royal Astron. Soc. Geophys. Jour., v. 36, p. 541-576.

Mortimer, C., and Rendic, N. S., 1975, Cenozoic studies in northernmost Chile: Geologische Rundschau, v. 64, p. 395-420.

Munoz, C. J., 1956, Chile, in Jenks, W. F., ed., Handbook of South American Geology: Geol. Soc. America Mem. 65, p. 191-214.

Ocola, L. C., and Meyer, R. P., 1973, Crustal structure from the Pacific basin to the Brazilian shield between 12° and 30° South latitude: Geol. Soc. America Bull., v. 84, p. 3387-3404.

Prince, R. A., 1974, Deformation in the Peru Trench, 6°-10°S (M.S. thesis): Corvallis, Oregon State University, 88 numb. leaves.

Prince, R. A., Resig, J. M., Kulm, L. D., and Moore, T. C., Jr., 1974, Uplifted turbidite basins on the seaward wall of the Peru Trench: Geol. Soc. America Bull., v. 86, p. 1639-1653.

Prince, R. A., and Kulm, L. D., 1975, Crustal rupture and the initiation of imbricate thrusting in the Peru-Chile Trench: Geol. Soc. America Bull., v. 86, p. 1639-1653.

Raitt, R. W., Fisher, R. L., and Mason, R. G., 1955, Tonga Trench: Geol. Soc. America Spec. Paper 62, p. 237-254.

Rosato, V. J., 1974, Peruvian deep-sea sediments: Evidence for continental accretion (M.S. thesis), Corvallis, Oregon State University, 93 numb. leaves.

Rosato, V. J., Kulm, L. D., and Derks, P. S., 1975, Surface sediments of the Nazca Plate: Pacific Science, v. 29, p. 117-130.

Ross, D. A., and Shor, G. G., Jr., 1965, Reflection profiles across the Middle America Trench: Jour. Geophys. Research, v. 70, p. 5551-5572.

Ruiz, C., 1965, Geologia y yacimientos metaliferos de Chile: Santiago, Inst. Invest. Geol., 305 p.

Rutland, R. W. R., 1971, Andean orogeny and ocean floor spreading: Nature, v. 233, p. 252-255.

Scholl, D. W., Von Huene, R., and Ridlon, J. B., 1968, Spreading of the ocean floor: undeformed sediments in the Peru-Chile Trench: Science, v. 159, p. 869-871.

Scholl, D. W., Christensen, M. N., Von Huene, R., and Marlow, M. S., 1970, Peru-Chile Trench sediments and sea-floor spreading: Geol. Soc. America Bull., v. 81, p. 1339-1360.

Seely, D. R., Vail, P. R., and Walton, G. G., 1974, Trench slope model, in Burk, C. A., and Drake, C. L., eds., The Geology of Continental Margins: New York, Springer-Verlag, p. 249-260.

Segerstrom, K., 1964, Quaternary geology of Chile: brief outline: Geol. Soc. America Bull., v. 75, p. 157-170.

Segerstrom, K., 1967, Geology and ore deposits of Central Atacama Province, Chile: Geol. Soc. America Bull., v. 78, p. 305-318.

Sillitoe, R. H., 1974, Tectonic segmentation of the Andes: implications for magmatism and metallogeny: Nature, v. 250, p. 542-545.

Stauder, W., 1968, Tensional character of earthquake foci beneath the Aleutian Trench with relation to sea-floor spreading: Jour. Geophys. Research, v. 73, p. 7693-7701.

Stauder, W., 1973, Mechanism and spatial distribution of Chilean earthquakes with relation to subduction of the oceanic plate: Jour. Geophys. Research, v. 78, p. 5033-5061.

Strobach, K., 1974, Curvature of island arcs and plate tectonics: Zeitschrift für Geophysick, Physica-Verlag, Würzburg.

Swift, S. A., and Carr, M. J., 1974, The segmented nature of the Chilean seismic zone: Physics of the Earth and Planetary Interiors, v. 9, p. 183-191.

Thompson, Sir C. W., and Murray, Sir J., 1895, Report on the scientific results of the voyage of H. M. S. Challenger during the years 1872-1876: A summary of the scientific results, first part: London.

Walcott, R. I., 1970, Flexural rigidity, thickness, and viscosity of the lithosphere: Jour. Geophys. Res., v. 75, p. 3941-3954.

Whitsett, R. A., 1976, Gravity measurements and their structural implications for the continental margin of southern Peru (Ph. D. thesis): Corvallis, Oregon State University, 82 numb. leaves.

Zeigler, J. M., Athearn, W. D., and Small, H., 1957, Profiles across the Peru-Chile Trench: Deep-Sea Research, v. 4, p. 238-249.

Zeil, W., 1964, Geologie von Chile: Berlin, Gert, Borntraeger, 231 p.

Zen, E., 1959, Mineralogy and petrography of marine bottom sediment samples off the coast of Peru and Chile: Jour. Sedimentary Petrology, v. 29, p. 513-539.

APPENDIX

APPENDIX I. Geologic Sample Data and Descriptions

Cruise[1]	Station Number and Type[2]		Latitude °S	Longitude °W	Water Depth (m)	Recovery (cm)	Description
FDRK	1	PC	32°57.3'	72°42.9'	5584	385	coarse, micaceous sand and clay
FDRK	2	PC	30°35.0'	72°37.3'	5850	80	clay in MG., coarse dark sand in cutter nose
FDRK	3	PC	30°34.4'	72°37.5'	5862	735	coarse sand turbidites overlying gray-green mud
FDRK	4	PC	27°28.2'	71°55.8'	6160	49	brown clay
FDRK	5	RD	26°59.7'	71°56.9'	6350		massive basalt
FDRK	7	RD	23°12.2'	71°21.5'	7600		pillow basalts volcanic breccia
FDRK	8	RD	23°15.7'	71°16.2'	8130		semi-consolidated mudstones and sandstones
FDRK	9	PC	23°14.7'	71°23.5'	7597	611	homogenous gray-green mud

APPENDIX I. Continued

Cruise[1]	Station Number and Type[2]	Latitude °S	Longitude °W	Water Depth (m)	Recovery (cm)	Description
Y73-6	73 PC	33°08.9'	72°44.3'	5412	277	gray-green mud and coarse dark sand
Y73-6	74 S	30°40.0'	71°44.0'	125	bag	olive green mud
Y73-6	75 G	30°38.3'	71°44.9'	135	14	olive green mud
Y73-6	77 FF	30°39'	72°41'	5425	79	brown clay over green clay
Y73-6	78 FF	30°39'	72°40'	5615	84	green clay and fine sand with brown clay at top
Y73-6	79 FF	30°39'	72°39'	5718	32	gray-green to brown clay and fine sand
Y73-6	80 FF	30°39'	72°39'	5671	< 5	lt. brown silty clay
Y73-6	81 PC	27°34.4'	71°51.3'	6118	1166	homogenous gray-green mud
Y73-6	82 PC	27°19.4'	71°20.0'	3063	222	homogenous gray-green mud

APPENDIX I. Continued

Cruise[1]	Station Number and Type[2]	Latitude °S	Longitude °W	Water Depth (m)	Recovery (cm)	Description
Y73-6	83 S	27°05.0'	70°59.8'	127	bag	dark med-fine sand
Y73-6	84 S	27°05.0'	71°00.5'	412	vial	sand
Y73-6	85 S	25°30.7'	70°42.0'	420	bag	dark silt, mud and shell fragments
Y73-6	86 PC	24°57.8'	70°57.6'	2925	128	rock fragments and lt. brown mud
Y73-6	87 FF	25°01.1'	71°25.5'		68	lt. brown and gray mud
Y73-6	88 RC	24°58.2'	70°52.3'	1638	10	lt. gray hard mud and rock bits
Y73-6	89 S	24°01.0'	70°33.5'	371		dark sand
Y73-6	90 S	24°01.9'	70°33.0'	193		dark sand
Y73-6	91 S	23°14.8'	70°37.3'	330		small amount of dark sand
Y73-6	92 S	23°14.5'	70°37.0'	210		sand

[1] FDRK = FDRAKE 1975, Scripps Institution of Oceanography
Y73-6 = YALOC 1973, Leg 6, Oregon State University

[2] PC = piston core
RD = rock dredge
RC = rock core
S = Shipek grab
G = gravity core
FF = free fall core